Table 1
Primer sequences used for RT-PCR analysis

Primer name	Forward	Reverse	Size of amplicon (bp)
CD44	CCCGAATTCATGGACAAGGT TTGGTGGCA	CCCGAATTCCTACACCCCAAT CTTCATAT	1095
GPDH	ACCACAGTCCATGCCATCAC	TCCACCACCCTGTTGCTGTA	450
CD44s	TCCCACTATGACACATATTGC	ACACCTTCTCCTACTGTTGAC	548
CD44v1	TCCCACTATGACACATATTGC	TTGTGAATTACCAAACCAAG	407
CD44v2	TCCCACTATGACACATATTGC	TGTATGAAGATGACTCTTGG	428
CD44v3	TCCCACTATGACACATATTGC	TCATTTGGCTTCCAGCCTGT	358
CD44v4	TCCCACTATGACACATATTGC	TTGTCTGAAGTAGTACTTCTG	424
CD44v5	TCCCACTATGACACATATTGC	ATGTGGGGTCTCCTCTTCAT	418
CD44v6	TCCCACTATGACACATATTGC	GGAGTCTTCACTTGGGGTGG	430
CD44v7	TCCCACTATGACACATATTGC	AATCGGTCCATGAAACATCCT	396
CD44v8	TCCCACTATGACACATATTGC	GTATTTGGAGCCGCAGTAGGC	373
CD44v9	TCCCACTATGACACATATTGC	GTCTTCGCCTTCTTCCAGCTC	362
CD44v10	TCCCACTATGACACATATTGC	TTCCATTGTGTCTGGATATTG	409
Albumin	AAGGCACCCCGATTACTCCG	TGCGAAGTCACCCATCACCG	608
TAT (tyrosine aminotransferase)	TACTCAGTTCTGCTGGAGCC	GCAAAGTCTCTAGAGAGGCC	471
CK8 (cytokeratin 8)	GGAGGTGGACCCCAACATCC	CCACAGACGTGTCTGAGATC	500
Transferrin	CCTGACAAAACGGTCAAATGGTGC	TAAAAACTCTGCTGCCACAGGC	251
C/EBPα	CGGGGCCGGCGCGGGCAAGG	GGGGAATTCTCACGCGCAGTT GCCCATGG	277
Cx32	ATGAACTGGACAGGTCTATA	TCAGCAGGCTGAGCATCGGT	854
HNF4	GGGGAATTCATGGACATGGC TGACTACAG	GGGGAATTCCTAGATGGCTTC CTGCTTGG	1368
CYP1A1	GATGCTGAGGACCAGGAAGACCGC	CAGGAGGCTGGACGAGAATGC	679
CYP3A1	CAGCTCTCACACTGGAAACCTGGG	TCGAGGATCTAAACAACCTGAC	689
CYP4A3	TCGAGGATCTAAACAACCTGAC	GGTTGTGATACCTTTGGGTATGG	573
c-kit	TCCGCTGCCCCCTGACAGAC	CTACATTTTCCCCATCAGTT	600
CD34	ATGCCGGTCCACAGGGGCGC	GACTCCCGAGGTAACCAATG	900
Thy1.1	ATGAACCCAGCCATCAGCGT	TGCCGCCACACTTGACCAGT	400
CK19	ATGACTTCCTATAGCTATCG	CACCTCCAGCTCGCCATTAG	340

with the modified PBS. After washing, anti-rat IgG microbeads for MACS (Miltenyi Biotec, Bergisch Gladbach, Germany) were added. Magnetic separation was done using a MidiMACS separation unit (Miltenyi Biotec) and the positive fraction was collected. This fraction was plated on dishes and cultured in modified DMEM. Some of the sorted and cultured cells were harvested and employed for analysis by RT-PCR.

3. Results

3.1. The expression of CD44 in SHs

Using a DNA microarray, the profile of gene expression was examined to clarify the difference between SHs and MHs. We selected 164 genes with much higher expression in SHs than in MHs. From these genes, we chose 16 that possessed the transmembrane sequence (Table 3) and RT-PCR analysis was performed to confirm whether the selected genes were specifically expressed in SHs. CD44 was one of the three genes (CD44, D6.1A, BRI3) restrictedly expressed in SHs (Fig. 1A). To examine the length of the mRNA of CD44, Northern blotting was carried out. Fig. 1B shows two bands of CD44 mRNA. As CD44 is known to have many variant forms, the expression of variant forms in SHs was examined by RT-PCR. As shown in Fig. 1C, both CD44s and CD44v6 were expressed in SHs. The lengths of mRNAs of CD44s and CD44v6 detected by Northern blotting corresponded to the 1384 and 1614 bp that were expected from the sequences, respectively.

Table 2
Antibodies

Antibodies	Company or producer	Dilution
Mouse anti-rat CD44	BD Biosciences PharMingen	1:1000
Rabbit anti-rat C/EBPα	Santa Cruz	1:400
Rabbit anti-rat CK19	Generous gift from Prof. Atsushi Miyajima[a]	1:1000
Mouse anti-rat Thy1.1	Serotec	1:500
Mouse anti-rat CD44v6	Generous gift from Dr Jonathan Sleeman[b]	1:100

[a] Molecular and Cellular Biology Institute, University of Tokyo, Tokyo, Japan.
[b] Institute of Genetics, Forschungszentrum Karlsruhe, Karlsruhe, Germany.

Table 3
Data from microarray

Name of the clone	Ratio[a]
Rat mRNA for D6.1A protein	6.6
Rat CD44 protein mRNA, complete cds	15.8
Rat heat stable CD24 mRNA, complete cds	24.7
Mouse brain cDNA, clone MNCb-2630, similar to Mouse G_1	12.8
Mouse mRNA for myeloid associated differentiation protein	16.3
Rat mRNA for HB2, complete cds	8.3
Mouse tetraspan TM4SF (Tspan-6) mRNA, complete cds	6.9
Mouse mRNA for adhesion protein RA175N, complete cds	5.3
Mouse mRNA for integrin alpha6 subunit	4.5
Mouse oncostatinM specific receptor mRNA, complete cds	4.7
KDEL receptor	4.3
KIAA0404	6.9
Mouse BRI3 mRNA, complete cds	4.4
Rat mRNA for E-cadherin, complete cds	10.7
Rat mRNA for caveolin	4.1
Rat mRNA for ad1-antigen	13.2

[a] Ratio: SH/MH.

Immunocytochemistry for CD44s showed that CD44s$^+$ cells, in which the cell membrane and cytoplasm were faintly stained, first appeared at day 3. The timing of the appearance corresponded to that of SH proliferation. As SHs proliferated and formed colonies, the distribution of the protein was restricted to the cell membrane and the staining became strong (Fig. 2D and F). Colonies that consisted of CD44s$^+$ cells showed a honeycomb-like appearance (Fig. 2F), but primary cultured MHs showed no CD44s positivity (Fig. 2A and B). NPCs such as liver epithelial cells (LECs) and stellate (Ito) cells around SH colonies were not stained for CD44s either (Fig. 2F, arrow). As previously reported [7,8], large and piled-up cells sometimes appeared in SH colonies and were morphologically MHs. As the cells in a colony increased in size, CD44s-positivity gradually decreased and it was hard to detect the positivity in the piled-up cells (Fig. 2G and H, asterisks). The time course of CD44s mRNA expression is shown in Fig. 3A. CD44s expression was clearly detected from day 3 and maintained for about

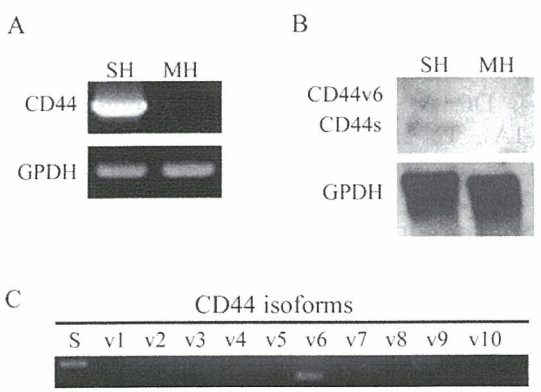

Fig. 1. Expression of CD44 in SHs cultured after cryopreservation. (A) Detection of transcript encoding CD44 by RT-PCR. Primer sets (Table I) for CD44 and GPDH were used. Total RNA was extracted from SHs that were cultured for 2 weeks after cryopreservation. Total RNA of MHs was also prepared from normal rat liver. The expected sizes of PCR products corresponding to CD44 and GPDH were 1095 and 450 basis pairs respectively. (B) Northern analysis of CD44 in SHs. 20 μg of total RNA was loaded into each lane. The filter was probed with alkaline phosphatase-linked DNA fragments specific for CD44 (upper) and GPDH (lower). Two bands of CD44 were observed in SHs. (C) Analysis of alternative splice variants of CD44 expressed in SHs. Transcripts encoding CD44 were amplified by RT-PCR using primer sets listed in Table 1. Two spliced variants (s and v6) of CD44 were expressed in SHs.

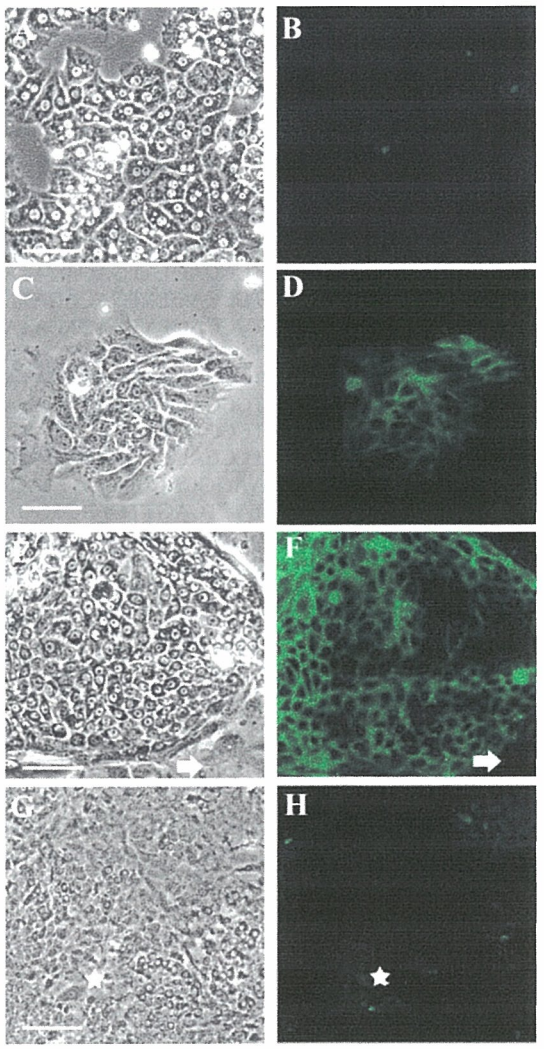

Fig. 2. Immunocytochemistry of CD44 on cultured SHs. Photographs show cell morphology under light microscopy (A, C, E, G) and immunostaining of CD44s (B, D, F, H; green). MHs isolated from a normal liver were cultured for 2 days (A and B). No expression of CD44s was observed in MHs. SHs were cultured for 5 (C and D), 18 (E and F) and 30 days (G and H). Expression of CD44 was initially observed at 3 days and reached the maximum around 18 days. CD44 disappeared from SHs by 30 days. Arrowheads indicate NPCs surrounding the SH colony (E and F). Asterisks also indicate the piled-up SHs (G and H). Expression of CD44s is faintly observed in a large, piled-up SH colony. Scale bars represent 140 μm for A, B, G, and H and 70 μm for C–F.

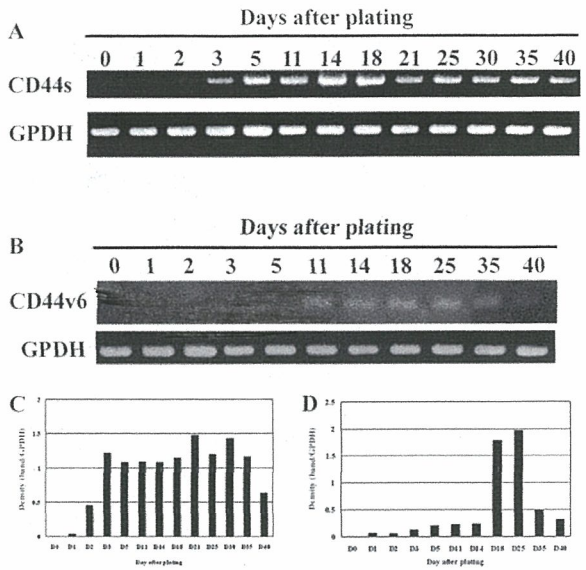

Fig. 3. Time course of CD44 expression in cultured SHs. (A) Detection of transcripts encoding CD44s by RT-PCR. SHs isolated from a normal liver were plated on culture dishes. Total RNA was extracted from cultured cells at each time point (0, 1, 2, 3, 5, 11, 14, 18, 21, 25, 30, 35, and 40 days). (B) Time course of CD44v6 expression in cultured SHs. Total RNA was extracted from cultured cells at each time point (0, 1, 2, 3, 5, 11, 14, 18, 21, 25, 30, 35, and 40 days). Primer set (Table 1) was used to detect expression of CD44v6. The expected size of the PCR product corresponding to CD44 was 430 bp. (C) Quantitation of CD44s and (D) CD44v6 expression in cultured SHs. The intensity of CD44 bands was measured by NIH image. Figure shows the density of the band normalized by GPDH. The expression of CD44s reached the maximum at around 14 days. On the other hand, maximum expression of CD44v6 was delayed compared to CD44s.

4 weeks. We also examined the expression of CD44v6 mRNA and protein in SHs. In analysis by RT-PCR, the expression of CD44v6 mRNA was detected later than that of CD44s (Fig. 3B). Immunostaining for CD44v6 showed that, in clusters of cells which were larger than SHs but smaller than binucleate MHs, the cell membranes were sometimes positive (Fig. 4).

3.2. CD44 expression with the maturation of SHs

To investigate whether the expression of CD44 was related to the maturation of SHs, Matrigel® was used to induce maturation. As shown in Fig. 5, when the cells were treated with Matrigel®, the expression of CD44s protein rapidly decreased and no expression was observed at day 4, whereas the expression of C/EBPα in MHs increased at day 4. CD44v6 expression was enhanced at day 2 and then decreased (Fig. 5). Although the expression of CD44s decreased at day 4 after the Matrigel® treatment, that of CD44v6 was not so much decreased at that time. Double staining for CD44s and C/EBPα in cultured SHs revealed that the cells, in which CD44s was strongly expressed in the cell membrane, did not possess C/EBPα $^{+}$-nuclei (Fig. 6A). In contrast, the

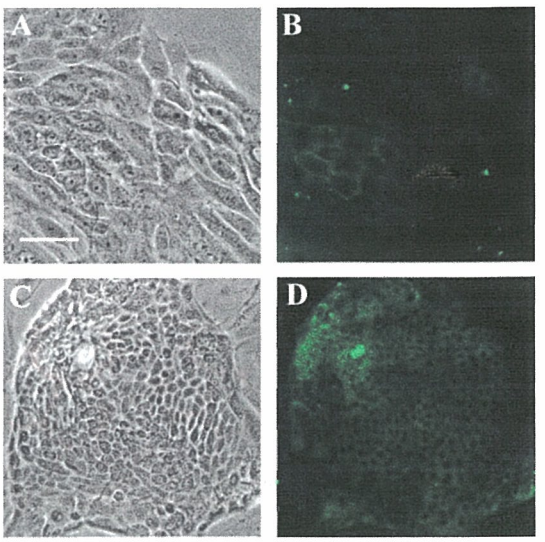

Fig. 4. Expression of spliced variant CD44v6 in cultured SHs. Photographs show cell morphology under light microscopy (A and C) and immunostaining of CD44v6 (B and D; green). SHs were cultured for 18 (A and B) and 30 days (C and D) after plating. CD44v6 appears on lateral surface of SHs.

cells in which C/EBPα protein was well expressed in the nuclei did not express CD44s in the cell membrane (Fig. 6B).

3.3. CD44 expression in vivo

Next, we examined the existence and distribution of CD44s $^{+}$ cells in the normal adult rat liver. BECs, lymphocytes, and fibroblastic cells in Glisson's capsule were positive for CD44s, whereas hepatocytes within hepatic lobules were not stained (Fig. 7A). As SHs were report-

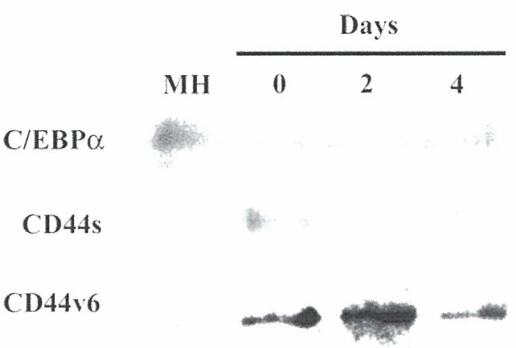

Fig. 5. Expression of C/EBPα CD44s, and CD44v6 in SHs treated with Matrigel. Immunoblotting of CD44s, CD44v6, and C/EBPα. Cell lysates were prepared from Matrigel-treated SHs and MHs. SHs were cultured for 0, 2, and 4 days after Matrigel treatment. Proteins separated by SDS-PAGE under reducing conditions were transferred onto nitrocellulose membranes followed by immunostaining with antibodies specific for C/EBPα (upper panel), CD44s (middle panel), and CD44v6 (lower panel). The expression of CD44s and CD44v6 disappeared as maturation occurred. However, the expression of CD44v6 was delayed compared to CD44s.

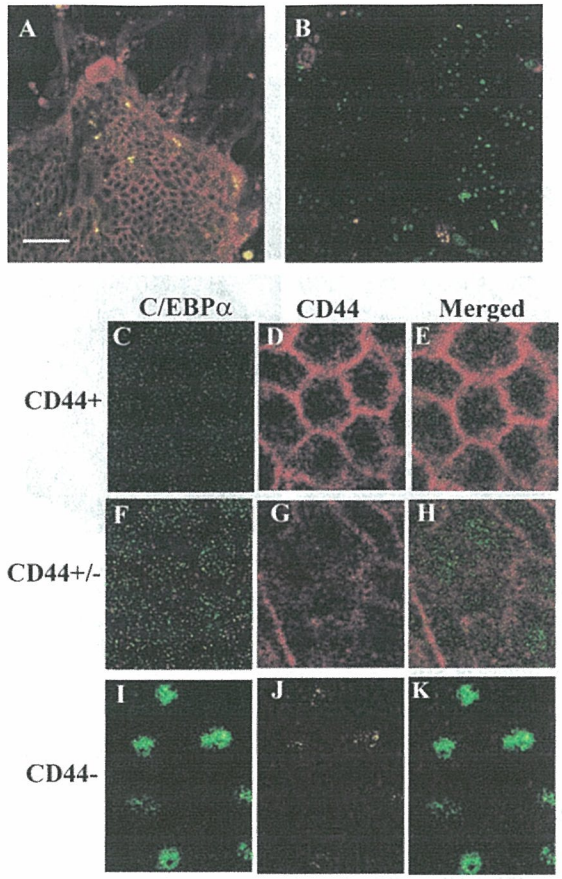

Fig. 6. Immunocytochemistry of CD44s and C/EBPα in cultured SHs. (A) Low-magnification photograph of SHs. Cells were doubly stained with a monoclonal antibody to CD44s (red) and polyclonal antibodies to C/EBPα (green). Expression of C/EBPα is only observed in matured SHs. (A) SHs were cultured for 21 and (B) 31 days after plating. Scale bars, 50 μm. (C–K) High-magnification photographs of SHs. Although CD44-positive cells did not express C/EBPα, negative cells had it in nuclei. Reciprocal expression of CD44s and C/EBPα is observed in cultured SHs.

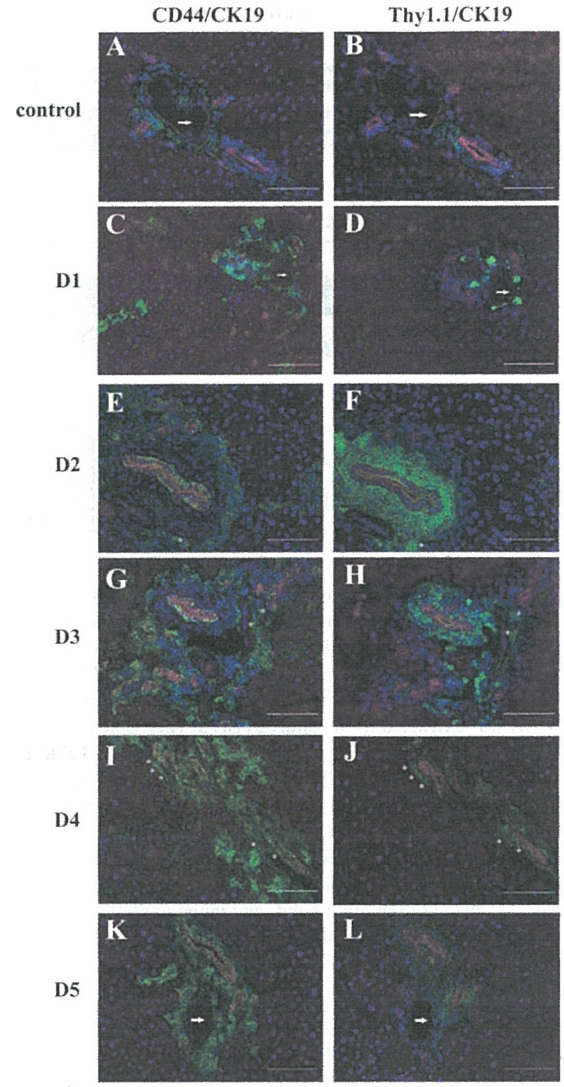

Fig. 7. Identification and localization of CD44s-positive cells in injured liver. Serial frozen sections of GalN-treated rat livers were doubly stained with antibodies to CD44s (green) and CK19 (red) (A, C, E, G, I and K) as well as Thy1.1 (green) and CK19 (red) (B, D, F, H, J and L). CK19 was used to identify BECs and Thy1.1 was used to identify oval cells. Nuclei were stained with DAPI (blue). No treatment: control rat liver; (A and B), D1; (C and D), D2; (E and F), D3; (G and H), D4; (I and J) and D5; (K and L): liver 1–5 days after treatment with GalN. Arrows show periportal region and asterisks show CD44s and Thy1.1 double-positive cells. Bile ducts are surrounded by CK-19-positive cells. Scale bars, 100 μm.

ed to appear in the rat liver severely injured by GalN [22], we examined whether those cells in the liver treated with GalN might express CD44. To further investigate the cell types that positively expressed CD44s, we carried out immunostaining using cell type-specific markers. Frozen liver sections from day 0 (control), and days 1–5 after GalN administration were double stained with antibodies to CD44s and CK19, which is a marker of BECs, and CK19 and Thy1.1, which is a marker of oval cells. Oval cells are known to be hepatic progenitor cells that appear in the GalN injury model. As shown in Fig. 7A, CD44s was expressed around the periportal area at day 0, but at days 3 and 4 CD44s$^+$ cells increased and appeared within liver lobules (Fig. 7G and I). At day 5 the number of CD44s$^+$ hepatocytes decreased compared to that at day 4 (Fig. 7K). At day 2 Thy1.1-positive cells were increased between Glisson's capsule and hepatocytes (Fig. 7F).

3.4. Sorting of CD44s$^+$ cells

As there were many CD44s$^+$/CK19$^-$ cells within liver lobules at day 4 after GalN treatment, we decided to isolate the CD44s$^+$ cells from the livers at that day. After CD44s$^+$ cells were sorted using MACS, the cells were cultured for 7 days. As shown in Table 4, about 1×10^6 CD44s$^+$ cells were separated from the GalN-treated rat, whereas few cells were separated from the normal rat. CD44$^+$ cells from the GalN-treated rat

Table 4
Recovery rate of sorted CD44 $^{+}$ cells from GalN-treated rat liver

Treatment	Number of rats	Initial number of cells[a] ($\times 10^6$)	Number of sorted cells ($\times 10^6$)	Recovery rate (%)
Control	3	179.0 ± 1.2	> 0.01	0
GalN	5	246.0 ± 0.9	1.32 ± 0.55	0.54

[a] MHs were depleted.

could form colonies, but the cells from the normal rat could not form any colonies. Seven days after plating, most colonies formed in the dishes consisted of SHs (Fig. 8A). In Fig. 8C, the expression of mRNAs for hepatocytes, oval cells and BECs is analyzed by RT-PCR. Many hepatic markers such as albumin, transferrin, CK8, connexin32, HNF4, C/EBPα, cytochrome P450 (CYP) 1A1, and CYP4A3 were expressed in sorted CD44 $^{+}$ cells, whereas there was

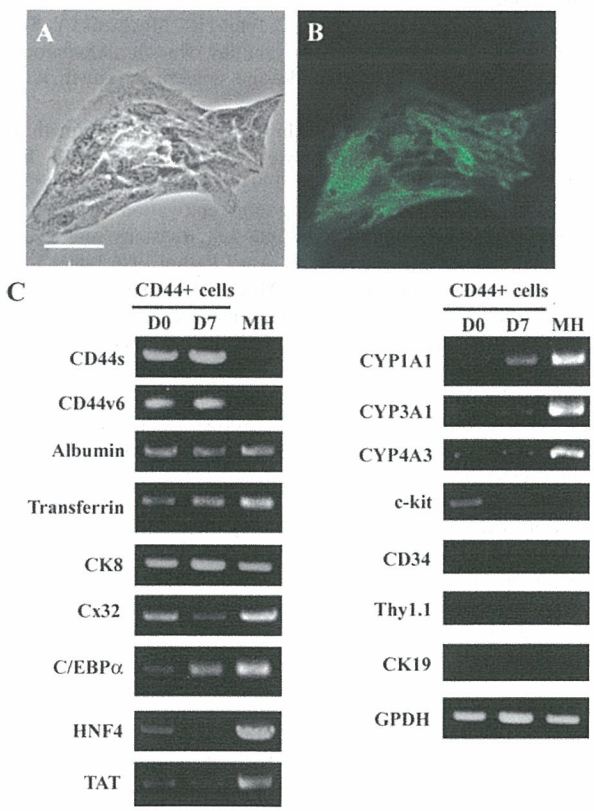

Fig. 8. Characterization of CD44-positive cells sorted from injured liver. (A) Expression of CD44s in the sorted cells. Photographs show cell morphology under light microscopy (left panel) and (B) immunostaining of CD44s in 7-day cultured cells. Scale bars, 70 μm. (C) Expression of hepatic markers in the sorted cells. Hepatic makers were detected by RT-PCR using primer sets. Total RNA was extracted from the sorted cells (day 0) and cultured CD44-positive cells (day 7). MHs were used as a positive control of hepatic maturation. Albumin, transferrin, CK8, Cx32, C/EBPα, HNF4, TAT, CYP1A1, CYP3A1, and CYP4A3 are markers for MHs; c-kit, CD34 for stem cells; Thy1.1 for oval cells, and CK19 for bile ductular cells.

no expression of markers for oval cells such as c-kit and Thy1.1, or for BECs such as CK19.

4. Discussion

In the present study, we examined the gene expression profiles of SHs and MHs to find SH-specific proteins. From our analyses, we confirmed that CD44s and CD44v6 were specifically expressed in cultured SHs but not in MHs. In in vivo studies using the GalN-injury model, CD44s $^{+}$ hepatocytes were observed in the periportal region. The GalN-induced liver injury model was established for activation of facultative liver stem cells, i.e. oval cells. Administration of GalN causes massive necrosis of hepatic parenchymal cells in the pericentral lesion [23], which leads to the activation, proliferation, and differentiation of oval cells into hepatocytes [24–26]. As shown in Fig. 7, Thy1.1 $^{+}$ oval cells appeared at days 2–4 in livers of GalN-treated rats. Although some Thy1.1 $^{+}$ cells possessing relatively large cytoplasms appeared very close to Glisson's capsule at days 3 and 4, MHs with Thy1.1 expression were never observed within lobules. Furthermore, some sorted Thy1.1 $^{+}$ cells expressed CD44s, but sorted CD44s $^{+}$ cells did not express Thy1.1 (data not shown). Nor could the sorted Thy1.1 $^{+}$ cells from day 2 form any SH colonies, whereas some Thy1.1 $^{+}$ cells from day 3 could form such colonies in our culture conditions (data not shown). These results suggested that some Thy1.1 $^{+}$ oval cells could initially differentiate into SHs and then into MHs in regeneration of the GalN-treated liver. On the other hand, our preliminary results showed that CD44s expression occurred in the expanded SH-like progenitor cells that appeared in the retrorsine/PH-treated rat liver [27,28]. In this model, oval cells did not appear. Within the GalN-liver lobules at days 3 and 4, many CD44s $^{+}$/Thy1.1 $^{-}$ cells appeared and most sorted CD44s $^{+}$ cells could form SH colonies in culture. Therefore, it is plausible that many CD44s $^{+}$ cells may come from MHs.

Expression of CD44s appeared at day 3 after plating of primary prepared SHs and increased at day 3 after GalN administration. These results suggested that CD44s expression could be up-regulated when the growth of SHs is stimulated. Therefore, although the mechanisms are at present unknown, situations where the replication of MHs is not sufficient to compensate for the loss of the cells or where SHs are free from the inhibitory signal(s) of MHs may act as a trigger for the cells, whose latent ability to be progenitors may be silenced.

A preliminary experiment provided a clue to the role of CD44 in SHs. Hyaluronic acid (HA) is a ligand for CD44. Although our data are preliminary, HA can induce the proliferation of SHs. When isolated hepatic

cells including SHs and NPCs were plated on HA-coated dishes, only SHs could proliferate to form colonies and the cells expressed CD44s. Although SECs are known to have HA receptors [29], they could not survive more than 1 week. Furthermore, the proliferating SHs on HA could not mature and the CD44s expression was maintained. In SHs, further analyses of the mechanisms by which CD44s can be induced only in SHs and how CD44 can signal the nucleus should be carried out.

The role of CD44v6 expression may be different from that of CD44s. CD44s may be related to the proliferation of SHs and to the maintenance of the capacity as progenitor cells, whereas CD44v6 may be related to their maturation because the expression of CD44v6 was delayed compared to that of CD44s in SHs and restricted to relatively large SHs. In addition, when SHs were treated with Matrigel®, the appearance of CD44v6 was delayed compared to that of CD44s. When SHs differentiated into MHs, the expression completely disappeared. CD44v6 was reported to be expressed in tumor cells, especially in metastasizing ones, and hematopoietic cells [30]. In the fetal rat liver, both CD44s and CD44v6 are expressed in hematopoietic precursor cells, including megakaryocytes [18]. In the present experiment, when SHs differentiated, the cell morphology changed from small to large and piled-up and CD44v6 transiently appeared in the cells. Therefore, the expression of CD44v6 may be related to the initiation of maturation.

In the present experiment, we clarified that CD44 was a specific marker of SHs. The expression of CD44 mRNA and protein was restricted to SHs, and was up-regulated at the time that SHs started to proliferate both in vitro and in vivo. The sorted CD44s$^+$ cells possessed hepatic markers, but no BEC or oval cell markers, except c-kit, were detected. Considering the present and preliminary results, we suggest that SHs are hepatic progenitor cells derived from MHs and some oval cells. Further experiments will be necessary to clarify the exact mechanisms by which their capability as progenitor cells is hidden and how the activation happens.

Acknowledgements

We thank Dr Jonathan P. Sleeman (Forschungszentrum Karlsruhe, Germany) for the generous gift of the anti-rat CD44v6 antibody, and Dr Atsushi Miyajima (University of Tokyo, Tokyo, Japan) for the generous gift of the anti-rat CK19 antibody. We thank Dr Toshimitsu Uede (University of Hokkaido, Japan) and Dr Yan-Jun Jia for suggestive discussions, Ms Chieko Doi, Ms Fumie Saito and Ms Minako Kuwano for technical assistance. We also thank Mr K. Barrymore for help with the manuscript.

This study was supported by grants from the Science and Technology Incubation Program in Advanced Regions, the Japan Science and Technology Agency and the Ministry of Education, Culture, Sports, Science and Technology, Japan; 14370393 and 17390353 for T. Mitaka, and Ministry of Health, Labour and Welfare, Health and Labour Sciences Research Grants, Research on Advanced Medical Technology for T. Mitaka.

Supplementary data

Supplementary data associated with this article can be found, in the online version, at doi:10.1016/j.jhep.2006.01.029.

References

[1] Mitaka T, Sattler CA, Sargen LM, Pitot HC. Multiple cell cycles occur in rat hepatocytes cultured in the presence of nicotinamide and epidermal growth factor. Hepatology 1991;13:21–30.
[2] Mitaka T, Mikami M, Sattler GL, Pitot HC, Mochizuki Y. Small cell colonies appear in the primary culture of adult rat hepatocytes in the presence of nicotinamide and epidermal growth factor. Hepatology 1992;16:440–447.
[3] Mitaka T, Kojima T, Mizuguchi T, Mochizuki Y. Growth and maturation of small hepatocytes isolated from adult liver. Biochem Biophys Res Commun 1995;214:310–317.
[4] Tateno C, Yoshizato K. Long-term cultivation of adult rat hepatocytes that undergo multiple cell divisions and express normal parenchymal phenotypes. Am J Pathol 1996;148:383–392.
[5] Mitaka T, Sattler GL, Pitot HC, Mochizuki Y. Characteristics of small cell colonies developing in primary cultures of adult rat hepatocytes. Virchows Arch B Cell Pathol Incl Mol Pathol 1992;62:329–335.
[6] Tateno C, Yoshizato K. Growth and differentiation in culture of clonogenic hepatocytes that express both phenotypes of hepatocytes and biliary epithelial cells. Am J Pathol 1996;148:1593–1605.
[7] Mitaka T, Sato F, Mizuguchi T, Yokono T, Mochizuki Y. Reconstruction of hepatic organoid by rat small hepatocytes and hepatic nonparenchymal cells. Hepatology 1999;29:111–125.
[8] Sugimoto S, Mitaka T, Ikeda S, Harada K, Ikai I, Yamaoka Y, et al. Morphological changes induced by extracellular matrix are correlated with maturation of rat small hepatocytes. J Cell Biochem 2002;1:16–28.
[9] Ikeda S, Mitaka T, Harada K, Sugimoto S, Hirata K, Mochizuki Y. Proliferation of rat small hepatocytes after long-term cryopreservation. J Hepatol 2002;37:7–14.
[10] Jalkanen S, Bargatze RF, de los Toyos J, Butcher EC. Lymphocyte recognition of high endothelium: antibodies to distinct epitopes of an 85–95 kDa glycoprotein antigen differentiallly inhibit lymphocyte binding to lymph node, mucosal, or synovial endothelial cells. J Cell Biol 1987;105:983–990.
[11] Stamenkovic I, Amiot M, Pesando JM, Seed B. A lymphocyte molecule implicated in lymph node homing is a member of the cartilage link protein family. Cell 1989;56:1057–1062.
[12] DeGrendele CH, Estess P, Siegelmen MH. Requirement for CD44 in activated T cell extravasation into an inflammatory site. Science 1996;278:672–675.
[13] Aruffo A, Stamenkovic I, Melnik M, Underhill CB, Seed B. CD44 is the principal cell surface receptor for hyaluronate. Cell 1990;61:1303–1313.

[14] Arch RK, Wirth M, Hofmann H, Ponta S, Herrlich P, Zöller M. Participation in normal immune response of a metastasis-inducing splice variant of CD44. Science 1992;257:182–185.
[15] Gunthert U, Hofmann M, Rudy W, Reber S, Zöller M, Haussmann S, et al. A new variant of glycoprotein CD44 confers metastatic potential to rat carcinoma cells. Cell 1991;65:13–24.
[16] Mackay CR, Terpe HJ, Stauder R, Marston WL, Stark H, Gunthert U. Expression and modulation of CD44 variant isoforms in humans. J Cell Biol 1994;124:71–82.
[17] Stauder R, Eisterer W, Thaler J, Gunthert U. CD44 variant isoforms in non-Hodgkin's lymphoma: a new independent prognostic factor. Blood 1995;85:2885–2899.
[18] Weber B, Rosel M, Arch R, Möller P, Zöller M. Transient expression of CD44 variant isoforms in the ontogeny of the rat: Ectoderm-, endoderm-, and mesoderm-derived cells express different exon combinations. Differentiation 1996;60:17–299.
[19] Salles G, Zain M, Jiang WM, Boussiotis VA, Shipp MA. Alternatively spliced CD44 transcripts in diffuse large-cell lymphomas: characterization and comparison with normal activated B cells and epithelial malignancies. Blood 1993;82:3539–3547.
[20] Seglen PO. Preparation of isolated rat liver cells. Methods Cell Biol 1976;13:29–83.
[21] Iizuka J, Katagiri Y, Tada N, Murakami M, Ikeda T, Sato M, et al. Introduction of an osteopontin gene confers the increase on B1 cell population and the production of anti-DNA autoantibodies. Lab Invest 1998;12:1523–1533.
[22] Dabeva MD, Hurston E, Shafriz DA. Transcription factor and liver-specific mRNA expression in facultative epithelial progenitor cells of liver and pancreas. Am J Pathol 1995;147:1633–1648.
[23] Decker K, Keppler D. Galactosamine hepatitis: key role of the nucleotide deficiency period in the pathogenesis of cell injury and cell death. Rev Physiol Biochem Pharmacol 1974;71:78–106.
[24] Lamire JM, Shiojiri N, Fausto N. Oval cell proliferation and the origin of small hepatocytes in liver injury induced by D-galactosamine. Am J Pathol 1991;139:535–552.
[25] Dabeva MD, Shafritz DA. Activation, proliferation, and differentiation of progenitor cells into hepatocytes in the D-galactosamine model of liver regeneration. Am J Pathol 1993;143:1606–1620.
[26] Dabeva MD, Alpini G, Hurston E, Shafritz DA. Models for hepatic progenitor cell activation. Proc Soc Exp Biol Med 1993;204:242–252.
[27] Gordon GJ, Coleman WB, Grisham JW. Temporal analysis of hepatocyte differentiation by small hepatocyte-like progenitor cells during liver regeneration in retrorsine-exposed rats. Am J Pathol 2000;157:771–786.
[28] Gordon GJ, Butz GM, Grisham JW, Coleman WB. Isolation, short-term culture, and transplantation of small hepatocyte-like progenitor cells from retrorsine-exposed rats. Transplantation 2002;73 (8):1236–1243.
[29] Goodison S, Urquidi V, Tarin D. CD44 cell adhesion molecules. J Clin Pathol Mol Pathol 1999;52:189–196.
[30] Smedsrød B, Pertoft H, Eriksson S, Fraser JRE, Laurent TC. Studies in vitro on the uptake and degradation of sodium hyaluronate in rat liver endothelial cells. Biochem J 1984;223:617–626.

0090-9556/06/3410-1667–1671$20.00
DRUG METABOLISM AND DISPOSITION
Copyright © 2006 by The American Society for Pharmacology and Experimental Therapeutics
DMD 34:1667–1671, 2006

Vol. 34, No. 10
8342/3142332
Printed in U.S.A.

Short Communication

Cytochrome P450 Expression of Cultured Rat Small Hepatocytes after Long-Term Cryopreservation

Received November 16, 2005; accepted July 19, 2006

ABSTRACT:

Small hepatocytes (SHs) are hepatic progenitor cells that can be cryopreserved for a long time. After thawing, the cells can proliferate and, when treated with Matrigel, they can differentiate into mature hepatocytes (MHs). In this study, we investigated whether cryopreserved SHs could express cytochromes P450 (P450s), whether P450 expression was induced by appropriate inducers, and whether P450 activities were measurable. 3-Methylcholanthrene (3-MC), phenobarbital (PB), pregnenolone-16α-carbonitrile (PCN), and ethanol were used as inducers for CYP1A, 2B, 3A, and 2E, respectively. Immunoblot analysis indicated that cryopreserved SHs constitutively expressed CYP1A1/2, CYP2E1, and CYP3A2 as much as 26 days after plating. Significant expression of CYP1A1/2 and 3A2 in the cells treated with Matrigel was induced by 3-MC and PCN, respectively. Although Matrigel did not up-regulate the enzymatic activity of CYP1A, CYP3A and CYP2E activities increased. Induction of CYP1A and CYP3A activities by each inducer was observed in cryopreserved cells treated with Matrigel. Although the expression of CYP2B1 could be detected in subcultured SHs treated with PB, it was not detected in cryopreserved SHs. The activity of NADPH-cytochrome P450 reductase was measured in both subcultured and cryopreserved SHs, although the activities in both were approximately 30% of that of MHs. Profiles of ^{14}C-testosterone metabolites were examined in cultured MHs and in cryopreserved SHs by high-performance liquid chromatography. Similar peaks for testosterone metabolites in MHs and SHs were observed in the same elution time. These results indicate that, although induction of CYP3A and 2B in cryopreserved SHs is inferior to that in subcultured ones, SHs can maintain the expression and activities of P450s after long-term cryopreservation.

Cytochromes P450 (P450) constitute a superfamily of monooxygenases that play a key role in either the detoxification or the metabolic activation of xenobiotics (Guengerich and MacDonald, 1990; Wrighton et al., 1992; Gonzalez and Gelboin, 1994). The P450s involved in xenobiotic metabolism are concentrated in liver cells. In vivo, many of the constitutive P450s are actually inducible by xenobiotics such as aromatic hydrocarbons, drugs, alcohol, etc. However, in traditional culture systems, it is very difficult to maintain the P450 activity of hepatocytes (Bissell and Guzelian, 1980). After cryopreservation of both rodent and human primary hepatocytes, rapid loss of hepatic differentiated functions, including P450 activity, has been reported in the cultured cells (Jackson et al., 1985; Loretz et al., 1989; Sun et al., 1990; Chesne et al., 1993; de Sousa et al., 1996; Swales et al., 1996; Garcia et al., 2003).

Small hepatocytes (SHs) have been identified as proliferating cells with hepatic characteristics (Mitaka et al., 1992, 1995; Tateno et al., 1996; Hino et al., 1999; Kon et al., 2006). We showed that a single SH could clonally proliferate and form flat colonies (Mitaka et al., 1999). It was also reported that maturation of the proliferating SHs was induced by the application of Engelbreth-Holm-Swarm sarcoma-derived matrix (Matrigel) (Sugimoto et al., 2002). Recently, SHs were shown to express several P450 proteins even after more than 1 month of culture (Miyamoto et al., 2005). In addition, the enzyme activities were induced and measured by the addition of appropriate inducers. Conversely, we reported that SHs could be cryopreserved for more than 6 months and that, even after thawing, the cells could maintain growth ability and hepatic differentiated functions (Ikeda et al., 2002).

In this study, we investigated whether cryopreserved SHs could express P450s, whether P450 expression was inducible, and whether P450 activities were measurable. The results showed that the protein expression of CYP1A1/2, CYP3A2, and CYP2E1 and the activities of CYP1A, CYP3A, CYP2E, and NADPH-cytochrome P450 reductase could be detected in the cells. Radiolabeled testosterone could be metabolized in long-term cultured cells and radioactive metabolites in cultured mature hepatocytes (MHs) were detected by high-performance liquid chromatography (HPLC).

Materials and Methods

Isolation and Culture of SHs. F344 rats (Sankyo Lab Service, Tokyo, Japan), weighing 170 to 240 g, were used. All animals received humane care, and

This study was supported by grants from the Science and Technology Incubation Program in Advanced Region, the Japan Science and Technology Agency, the Ministry of Education, Culture, Sports, Science and Technology, Japan (14370393, 17390353) to T.M., and Ministry of Health, Labour and Welfare, Health and Labour Sciences Research Grants, Research on Advanced Medical Technology to T.M.

Article, publication date, and citation information can be found at http://dmd.aspetjournals.org.

doi:10.1124/dmd.105.008342.

ABBREVIATIONS: P450, cytochrome P450; DMEM, Dulbecco's modified Eagle's medium; DMSO, dimethyl sulfoxide; EtOH, ethanol; HPLC, high-performance liquid chromatography; KH, Krebs-Henseleit; 3-MC, 3-methylcholanthrene; MH, mature hepatocyte; PB, phenobarbital; PCN, pregnenolone-16α-carbonitrile; SH, small hepatocyte.

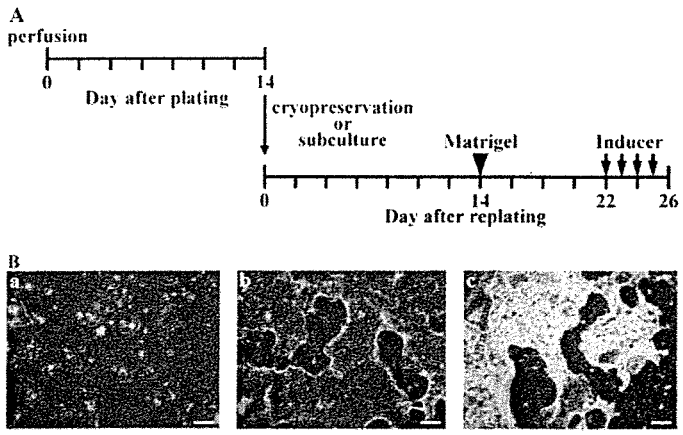

FIG. 1. A, the experimental schedule. SHs were isolated from a rat liver and cultured in modified DMEM. SH colonies were detached from the culture dishes at 14 days after plating and immediately replated or cryopreserved at −80°C for more than 1 month. One day after replating, the medium was replaced with serum-free DMEM containing 1% DMSO. Fourteen days later, the cells were overlaid with Matrigel. Arrows indicate the timing of the P450 inducer treatment. Cells at 26 days were harvested from dishes and examined for P450 expression and enzyme activities. B, phase-contrast micrographs of cryopreserved SHs at days 2 (a) and 21 (b). At day 7 after Matrigel treatment, most cells in colonies were piled up (c). All photos are the same magnification. Scale bar, 300 μm.

the experimental protocol was approved by the Committee of Laboratory Animals according to Sapporo Medical University guidelines. Hepatic cells were isolated by the two-step collagenase perfusion method. Details of the isolation and culture procedure for SHs were described previously (Mitaka et al., 1999). Finally, 6×10^4 viable cells/cm^2 were seeded on a 100-mm dish and cultured in Dulbecco's modified Eagle's medium (DMEM; Sigma Chemical Co., St. Louis, MO) supplemented with 20 mM HEPES, 25 mM $NaHCO_3$, 30 mg/l L-proline, 10% fetal bovine serum (HyClone, Logan, UT), 10 mM nicotinamide (Katayama Chemical Co., Osaka, Japan), 1 mM ascorbic acid 2-phosphate (Wako Pure Chemical Co., Tokyo, Japan), 10 ng/ml epidermal growth factor (Collaborative Research Inc., Lexington, MA), 0.5 mg/l insulin, 10^{-7} M dexamethasone, and antibiotics. After 4 days of culture, 1% dimethyl sulfoxide (DMSO; Aldrich Chemical Co., Milwaukee, WI) was added to the medium.

Subculture and Cryopreservation of Small Hepatocyte Colonies. As previously reported (Mitaka et al., 1999; Ikeda et al., 2002), colonies consisting of 30 to 50 cells were observed at day 14 after plating. To collect SHs, the colonies were detached from dishes and immediately replated or cryopreserved at −80°C until use (Fig. 1A). SH colonies ($3–5 \times 10^3$ colonies/60-mm dish) were replated on dishes coated with rat-tail collagen. One day after replating, the medium was replaced with serum-free modified DMEM supplemented with 1% DMSO. Fourteen days after replating, some dishes were treated with Matrigel (1 mg/dish; Becton Dickinson, Bedford, MA).

Immunoblots for P450 Proteins. 3-Methylcholanthrene (3-MC; Wako Pure Chemical Co.), phenobarbital (PB; Wako Pure Chemical Co.), pregnenolone-16α-carbonitrile (PCN; Sigma Chemical Co.), and ethanol (EtOH; Katayama Chemical Co.) were used as inducers for CYP1A, 2B, 3A, and 2E, respectively. Eight days after Matrigel treatment, fresh medium containing the inducer (5 μM 3-MC, 2 mM PB, 2 μM PCN, or 100 mM EtOH) was added. To enhance the P450 expression, the medium containing each inducer was renewed every day for 3 consecutive days before harvest (Fig. 1A).

For immunoblots, the dishes were washed with PBS twice and then treated with 1 ml of lysis buffer (10 mM Tris-HCl, pH 8.0, 5 mM EDTA, 150 mM NaCl, 1% Triton X-100, 5 μg/ml leupeptin, 5 μg/ml pepstatin A) for 1 h at 4°C. The cells were scraped and used for protein extraction. Samples (15 μg/lane) were separated by SDS-polyacrylamide gel electrophoresis. Rabbit anti-CYP1A2, anti-CYP3A2, goat anti-CYP2B1, and anti-CYP2E1 (Daiichi Pure Chemical Co., Tokyo, Japan) antibodies were used for immunoblots. The details of the method were described previously (Miyamoto et al., 2005).

Enzyme Activity of P450s. For the measurement of P450 enzyme activity, the cells were washed with KH buffer (0.96% Krebs-Henseleit buffer powder, 2.5 mM $CaCl_2 \cdot 2H_2O$, 25 mM $NaHCO_3$, pH 7.5) twice at 37°C. After addition of 1.5 ml of KH buffer containing the substrates, 3 μM ethoxyresorufin, 125 μM testosterone, or 300 μM chlorzoxazone, the cells were incubated for 1 h at 37°C. The reaction reagents were collected and centrifuged at 12,000*g* for 10 min at 4°C. Then the supernatants were collected and dosed with 250 μl of methanol containing 10 μg/ml phenacetin to stop the reaction. Samples were kept at −80°C until use. Metabolites catalyzed by each P450 were fluorometrically measured according to the method of Burke and Mayer (1974) with some modifications (Miyamoto et al., 2005). P450 activities were determined by 7-ethoxyresorufin *O*-deethylation (CYP1A), testosterone-6β-hydroxylation (CYP3A), and chlorzoxazone 6-hydroxylation (CYP2E).

NADPH-Cytochrome P450 Reductase Activity. Activity of NADPH-cytochrome P450 reductase was measured by the method of Yukawa et al. (1983).

Profiles of ^{14}C-Testosterone Metabolites. SHs treated with Matrigel at day 22 and cultured MHs at day 1 were examined. MHs were seeded on a 100-mm dish and cultured in DMEM containing 10% fetal bovine serum. The cells were washed with KH buffer twice at 37°C. After addition of 1.5 ml of KH buffer containing 125 μM ^{14}C-testosterone (Amersham Biosciences Inc., Piscataway, NJ) to the dish, the cells were incubated for 1 h at 37°C. The reaction reagents were filtered by centrifugation (5000*g*, 5 min, 4°C) with an UltraFree-CL filter (0.45 μm; Millipore, Billerica, MA), and 100 μl was analyzed. Metabolites were detected using HPLC (LC-10ADvp; Shimadzu, Kyoto, Japan) with a Cosmosil 5C18-AR column (4.6 × 250 mm; Nacalai Tesque, Kyoto, Japan) and a radioactivity detector (FLO-ONE 525TR; Packard Instruments, Meriden, CT). The column temperature was set at 40°C and the UV detector was set at 240 nm. The mobile phase was water/tetrahydrofuran (5:1 v/v) as solvent A and methanol as solvent B. Gradient conditions were 0 to 20 min, 20 to 30% B (linear gradient); 20 to 20.5 min, 30 to 70% B (linear gradient); 20.5 to 24 min, 70% B; 24 to 25 min, 70 to 20% B (linear gradient); 25 to 30 min, 20% B. The flow rate was 1 ml/min.

Statistical Analysis. Statistical analysis was performed using Tukey's honestly significant difference test. A p value of <0.05 was considered significant.

Results and Discussion

SHs began dividing from day 3 and rapidly proliferated to form colonies. At day 14 after plating, many colonies consisting of 30 to 50 cells were detached from dishes. The colonies were replated on new dishes or cryopreserved for more than 1 month. Most subcultured colonies could attach, but only about 60% of thawed colonies could attach to collagen-coated dishes (Ikeda et al., 2002). Attached cells proliferated to form a large monolayer colony (Fig. 1B-b). Other types of cells, such as liver epithelial cells and stellate cells, also survived cryopreservation but were few in number. As reported previously (Sugimoto et al., 2002), when SH colonies were treated with Matrigel, the shape of proliferating SHs changed from flat to rising/piled-up and size from small to large. The alteration resulted in the differentiation of SHs into MHs. The cells could express not only tryptophan 2,3-dioxygenase and serine dehydratase but also liver-enriched transcription factors such as hepatocyte nuclear factors 4α and 6, and CCAAT/enhancer binding protein α and β, which are known to be restrictedly expressed in highly differentiated hepatocytes (Sugimoto et al., 2002). Expression of P450 protein and activity was also demonstrated in the SHs treated with Matrigel (Miyamoto et al., 2005). Therefore, we first examined the effect of Matrigel treatment on the morphology of cryopreserved SHs. As shown in Fig. 1B-c, the shape of most cells in colonies changed from flat to rising/piled-up within 1 week. This result was coincident with that of subcultured SHs (Miyamoto et al., 2005). We then examined the expression of P450 proteins by immunoblotting. As shown in Fig. 2, A and B, CYP1A1/2 and CYP3A2 were constitutively expressed and not induced by Matrigel in both subcultured and cryopreserved SHs. Expression of CYP2B1 was detected in subcultured SHs treated with PB but not in cryopreserved SHs. In contrast, CYP2E1 was detected in subcultured SHs treated with Matrigel but constitutively expressed in cryopreserved ones.

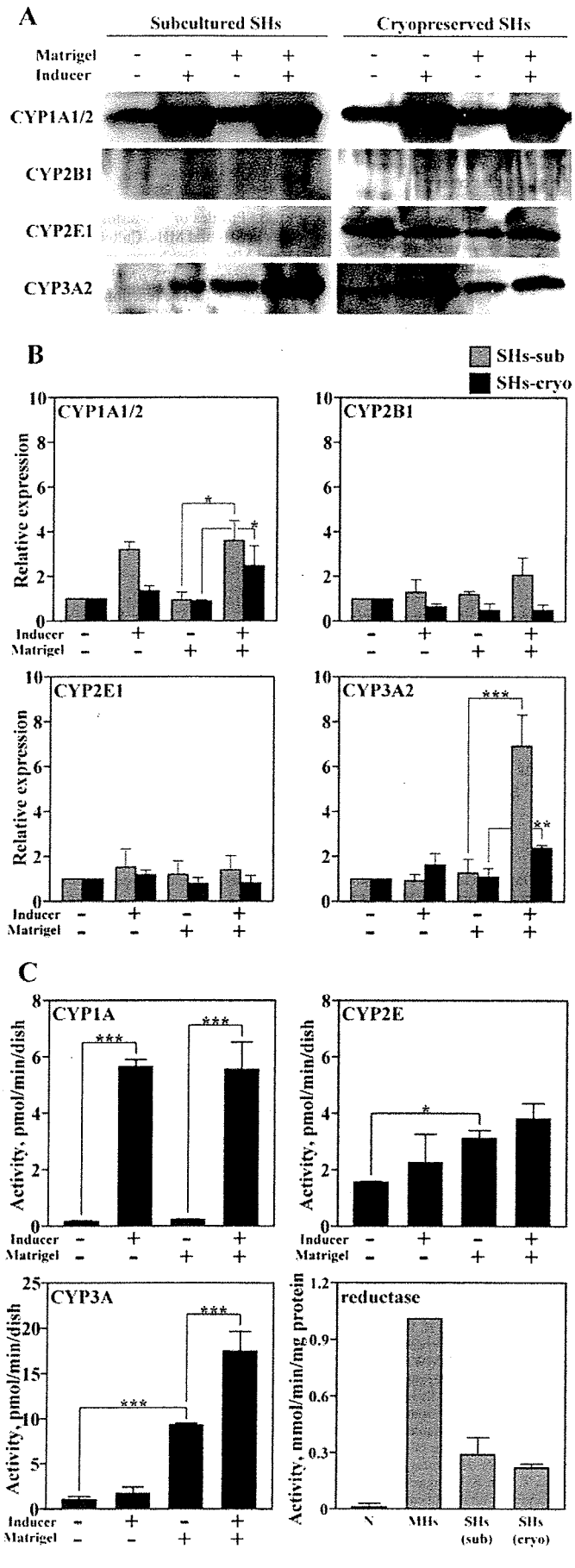

When SHs were treated with 3-MC and PCN for 4 days, CYP1A1/2 and CYP3A2, respectively, were induced in the cells with Matrigel. However, this induction was not observed in the cells without Matrigel. As shown in Fig. 2B, the pattern of CYP1A1/2 and CYP3A2 induction showed similarity between subcultured (3.6-fold and 6.9-fold) and cryopreserved (2.4-fold and 2.4-fold) SHs. CYP3A1 is known to be the dominant 3A after the induction. The cross-reactivity of the antibody between 3A1 and 3A2 is not clear. Therefore, the induced 3A may be 3A1 in the present experiment. Induction of CYP2E1 by EtOH was not detected in either subcultured or cryopreserved SHs.

Next, we investigated whether cryopreserved SHs could have P450 enzymatic activities. As shown in Fig. 2C, activities of 7-ethoxyresorufin *O*-deethylation (CYP1A), testosterone-6β-hydroxylation (CYP3A), chlorzoxazone 6-hydroxylation (CYP2E), and testosterone 16β-hydroxylation (CYP2B) were measured in cryopreserved SHs. In the cells without Matrigel, the activities of CYP1A and CYP3A were quite low and that of CYP2B was not detected. Enzyme activities of CYP2E and CYP3A were induced in the cells with Matrigel (2.0-fold and 8.7-fold, respectively). When SHs were treated with inducers, induction of CYP1A activity by 3-MC was observed (32-fold without Matrigel and 23-fold with Matrigel). Induction of CYP3A activity was observed in the cells with Matrigel (1.9-fold), whereas SHs without Matrigel did not show induction of CYP3A. Despite EtOH treatment, CYP2E activity did not show any significant difference between the cells with and without Matrigel. Very low activity of CYP2B was observed only in the cells with both Matrigel and PB (data not shown). There was a close relationship between the protein expression and the enzymatic activity of each P450, although some discrepancies were found; CYP3A2 protein was not adequately induced in the cells with Matrigel, and the CYP1A activity was low, although the protein was expressed. To investigate the causes of these discrepancies, we examined the activity of NADPH-cytochrome P450 reductase in SHs. As shown in Fig. 2C, the activity was observed in both subcultured and cryopreserved SHs, although measured activity was approximately 0.3-fold that of MHs. The results indicated that the reductase activity might affect P450 activity.

Although we did not detect expression and activity of CYP2B in the cryopreserved SHs, the present experiment and a previous one (Miyamoto et al., 2005) showed that subcultured SHs could express it. To determine the reason, the expression of CYP2B1 in cryopreserved SHs was measured during culture. At the time of thawing, the cells

FIG. 2. A, immunoblots for P450 proteins induced by various P450 inducers in subcultured SHs and cryopreserved SHs treated with or without Matrigel. 3-MC, PB, EtOH, and PCN were used for CYP1A1/2, CYP2B1, CYP2E1, and CYP3A2, respectively. Samples (15 μg/lane) were separated by 10% SDS-polyacrylamide gel electrophoresis. Relative expression of each P450 was estimated from immunoblots and is presented in B. C, P450 enzymes and NADPH-cytochrome P450 reductase activity. Activities of P450 proteins were induced by various inducers in cryopreserved SHs treated with or without Matrigel. The cells were exposed to KH buffer containing the substrate, 3 μM ethoxyresorufin (CYP1A), 125 μM testosterone (CYP3A), or 300 μM chlorzoxazone (CYP2E) for 1 h at 37°C, and reaction reagent was collected. Resorufin, 6β-hydroxytestosterone, and 6-hydroxychlorzoxazone were detected as metabolites. Activities of P450s (pmol/min/dish) were calculated. Activity of NADPH-cytochrome P450 reductase was measured in MHs, subcultured SHs, and cryopreserved SHs. Protein (0.1 mg) was added to buffer (1 ml) containing 0.1 M Tris-HCl (pH 7.5), 25 μM cytochrome *c*, and 0.1 mM NADPH. Reduction of cytochrome *c* was detected with a spectrophotometer (550 nm) and activity was estimated as units/mg (mM/min/mg protein). "N" indicates no protein. Excluding reductase activity of MHs, all data are means ± S.D. from three different experiments. Asterisks indicate significant induction with the inducer or Matrigel (*, $p < 0.05$; **, $p < 0.01$; ***, $p < 0.001$).

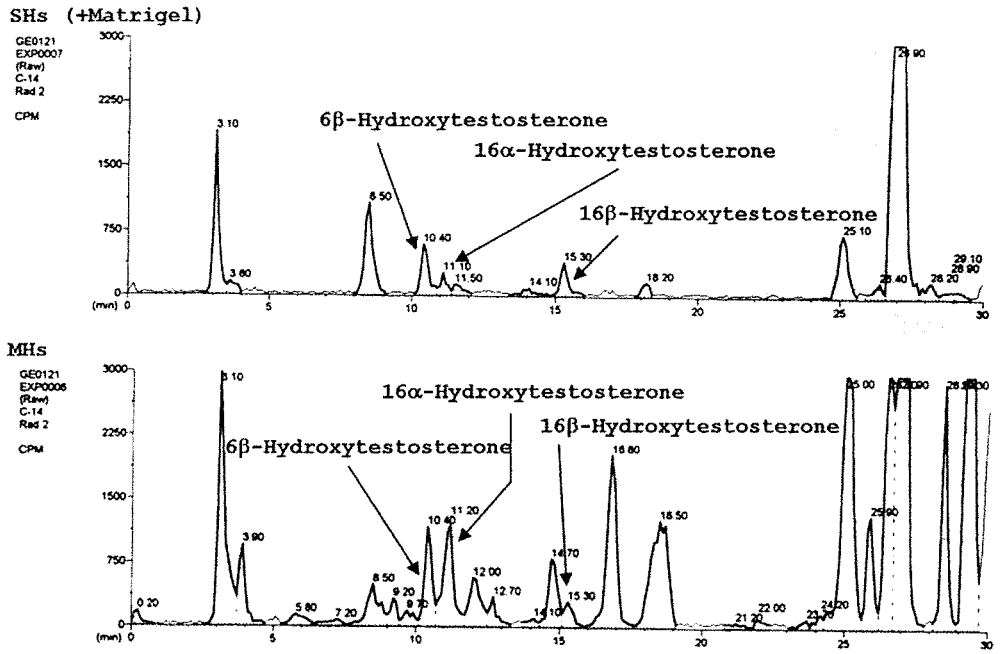

FIG. 3. Profiles of ^{14}C-testosterone metabolites in SHs and MHs. Cultured SHs at day 22 and MHs at day 1 were incubated in KH buffer containing 125 μM ^{14}C-testosterone for 1 h at 37°C. The reaction reagents were analyzed using HPLC. The main metabolites of testosterone catalyzed by P450s are indicated by arrows.

possessed the protein, but the expression rapidly decreased with time in culture. Within 3 days, the enzyme was not detected in the cells (data not shown). Further experiments are necessary to clarify the mechanism of the loss.

Next, we investigated the profiles of testosterone metabolites in SHs treated with Matrigel. As shown in Fig. 3, several metabolites of testosterone were indicated as peaks in both MHs and SHs; for example, 6β-hydroxytestosterone, 16α-hydroxytestosterone, and 16β-hydroxytestosterone. Although the heights of the peaks were relatively lower in SHs than in cultured MHs and some metabolites were not detected in SHs, testosterone could be sequentially metabolized in the cryopreserved SHs as effectively as in cultured MHs. The quite low peak of 16β-hydroxytestosterone in SHs was due to the low expression of CYP2B. The results correlated with those of both protein and enzyme activity experiments.

In the present study, we showed that cryopreserved SHs could maintain the inducibility of both P450 proteins and their enzyme activities. Until now, to supply hepatocytes used for pharmacological and pharmaceutical investigations, it has been necessary to isolate MHs for every experiment because there are few cell lines possessing hepatic differentiated functions, especially P450 enzyme activities. In addition, the number of obtainable cells depends on the number of cells in the individual because a method for proliferating hepatocytes with differentiated functions has not been established. However, by using SHs, these problems may be resolved because SHs can be isolated from adult rodents, can continue proliferating, and can be cryopreserved for a long time. Whenever hepatocytes are required, cryopreserved SHs may be thawed and plated on dishes. After the SHs proliferate and reach the required number, maturation of the cells is easily induced by Matrigel. Although improvements of the culture conditions are necessary, e.g., an increase of CYP2B expression, we think that cryopreserved SHs may be very useful for pharmacological and toxicological studies.

Acknowledgments. We thank Drs. Yan-Jun Jia and Hideki Oshima for suggestive discussions, and Makiyo Uchida, Chieko Doi, and Minako Kuwano for technical assistance.

Department of Pathophysiology, Cancer Research Institute (H.O., J.K., T.M.) and First Department of Surgery (S.M.), Sapporo Medical University School of Medicine, Sapporo, Japan; and Daiichi Pure Chemical Co. Ltd., Tokai, Ibaraki, Japan (Y.O., S.N.)

HIDEKAZU OOE
JUNKO KON
SHIGEKI MIYAMOTO
YOSHIYASU OZONE
SHIN-ICHI NINOMIYA
TOSHIHIRO MITAKA

References

Bissell DM and Guzelian PS (1980) Phenotypic stability of adult rat hepatocytes in primary monolayer culture. *Ann NY Acad Sci* **349**:85–98.

Burke MD and Mayer RT (1974) Ethoxyresorufin: direct fluorimetric assay of a microsomal O-dealkylation which is preferentially inducible by 3-methylcholanthrene. *Drug Metab Dispos* **2**:583–588.

Chesne C, Guyomard C, Fautrel A, Poullain MG, Fremond B, De Jong H, and Guillouzo A (1993) Viability and function in primary culture of adult hepatocytes from various animal species and human beings after cryopreservation. *Hepatology* **18**:406–414.

de Sousa G, Langouet S, Nicolas F, Lorenzon G, Placidi M, Rahmani R, and Guillouzo A (1996) Increase of cytochrome P4501A and glutathione transferase transcripts in cultured hepatocytes from dogs, monkeys and humans after cryopreservation. *Cell Biol Toxicol* **12**:351–358.

Garcia M, Rager J, Wang Q, Strab R, Hidalgo IJ, Owen A, and Li J (2003) Cryopreserved human hepatocytes as alternative in vitro model for cytochrome p450 induction studies. *In Vitro Cell Dev Biol Anim* **39**:283–287.

Gonzalez FJ and Gelboin HV (1994) Role of human cytochromes P450 in the metabolic activation of chemical carcinogens and toxins. *Drug Metab Rev* **26**:165–183.

Guengerich FP and MacDonald TL (1990) Mechanisms of cytochrome P-450 catalysis. *FASEB J* **4**:2453–2459.

Hino H, Tateno C, Sato H, Yamasaki C, Katayama S, Kohashi T, Aratani A, Asahara T, Dohi K, and Yoshizato K (1999) A long-term culture of human hepatocytes which show a high growth potential and express their differentiated phenotypes. *Biochem Biophys Res Commun* **256**:184–191.

Ikeda S, Mitaka T, Harada K, Sugimoto S, Hirata K, and Mochizuki Y (2002) Proliferation of rat small hepatocytes after long-term cryopreservation. *J Hepatol* **37**:7–14.

Jackson BA, Davies JE, and Chipman JK (1985) Cytochrome P-450 activity in hepatocytes following cryopreservation and monolayer culture. *Biochem Pharmacol* **34**:3389–3391.

Kon J, Ooe H, Oshima H, Kikkawa Y, and Mitaka T (2006) Expression of CD44 in rat hepatic progenitor cells. *J Hepatol* **45**:90–98.

Loretz LJ, Li AP, Flye MW, and Wilson GE (1989) Optimization of cryopreservation procedures for rat and human hepatocytes. *Xenobiotica* **19**:489–498.

Mitaka T, Kojima T, Mizuguchi T, and Mochizuki Y (1995) Growth and maturation of small hepatocytes isolated from adult rat liver. *Biochem Biophys Res Commun* **214**:310–317.

Mitaka T, Mikami M, Sattler GL, Pitot HC, and Mochizuki Y (1992) Small cell colonies appear in the primary culture of adult rat hepatocytes in the presence of nicotinamide and epidermal growth factor. *Hepatology* **16**:440–447.

Mitaka T, Sato F, Mizuguchi T, Yokono T, and Mochizuki Y (1999) Reconstruction of hepatic organoid by rat small hepatocytes and hepatic nonparenchymal cells. *Hepatology* **29**:111–125.

Miyamoto S, Hirata K, Sugimoto S, Harada K, and Mitaka T (2005) Expression of cytochrome P450 enzymes in hepatic organoid reconstructed by rat small hepatocytes. *J Gastroenterol Hepatol* **20**:865–872.

Sugimoto S, Mitaka T, Ikeda S, Harada K, Ikai I, Yamaoka Y, and Mochizuki Y (2002) Morphological changes induced by extracellular matrix are correlated with maturation of rat small hepatocytes. *J Cell Biochem* **87:**16–28.

Sun EL, Aspar DG, Ulrich RG, and Melchior GW (1990) Cryopreservation of cynomologus monkey (Macaca fascicularis) hepatocytes for subsequent culture and protein synthesis studies. *In Vitro Cell Dev Biol* **25:**147–150.

Swales NJ, Luong C, and Caldwell J (1996) Cryopreservation of rat and mouse hepatocytes. I. Comparative viability studies. II. Assessment of metabolic capacity using testosterone metabolism. *Drug Metab Dispos* **24:**1224–1230.

Tateno C and Yoshizato K (1996) Long-term cultivation of adult rat hepatocytes that undergo multiple cell divisions and express normal parenchymal phenotypes. *Am J Pathol* **148:**383–392.

Wrighton SA and Stevens JC (1992) The human hepatic cytochromes P450 involved in drug metabolism. *Crit Rev Toxicol* **22:**1–21.

Yukawa O, Nagatsuka S, and Nakazawa T (1983) Reconstitution studies on the involvement of radiation-induced lipid peroxidation in damage to membrane enzymes. *Int J Radiat Biol Relat Stud Phys Chem Med* **43:**391–398.

Address correspondence to: Dr. Toshihiro Mitaka, Department of Pathophysiology, Cancer Research Institute, Sapporo Medical University School of Medicine, South-1, West-17, Chuo-Ku, Sapporo 060-8556, Japan. E-mail: tmitaka@sapmed.ac.jp

Original Paper

European Surgical Research

Eur Surg Res 2006;38:522–532
DOI: 10.1159/000096292

Received: June 8, 2006
Accepted after revision: August 2, 2006
Published online: October 16, 2006

Portal Blood Flow Regulates Volume Recovery of the Rat Liver after Partial Hepatectomy: Molecular Evaluation

T. Nobuoka[a] T. Mizuguchi[a] H. Oshima[a] T. Shibata[a] Y. Kimura[a] T. Mitaka[b] T. Katsuramaki[a] K. Hirata[a]

[a]Department of Surgery I, Sapporo Medical University Hospital, Sapporo, and [b]Department of Pathophysiology, Cancer Research Institute, Sapporo Medical University School of Medicine, Sapporo, Japan

Key Words
CCAAT/enhancer-binding proteins · Cardiotropin-1 · Cyclins · Hepatic tissue blood flow · Liver regeneration

Abstract
Background/Aim: Liver regeneration is a finely tuned process that is closely regulated by multiple cell cycle steps. Although the portal blood flow affects liver regeneration, the molecular mechanism by which the blood flow regulates gene expression and liver function is largely unknown. The aim of this study was to investigate the molecular effect of portal blood flow on hepatocyte proliferation and gene regulation during liver regeneration. ***Materials and Methods:*** We developed a simple surgical rat model to investigate the relation between portal blood flow and liver regeneration by partially ligating the portal trunk with 8-0 Proline sutures under microscopy to reduce the blood flow by 40%. We investigated recovery of liver volume, DNA synthesis, and gene expression associated with cell cycle regulators, comparing partially hepatectomized (PH) rats without (PH group; n = 30) and with partial portal ligation (PHPL group; n = 30) for 7 days after the operation. ***Results:*** The hepatic tissue blood flow and the recovery ratio between liver weight and body weight in the PHPL group were significantly lower than in the PH group after hepatectomy. The peak 5-bromo-2′-deoxyuridine labeling index in the PHPL group was delayed and weak compared with the PH group. The expression of CT-1 and cyclin D, E, and B mRNAs indicated that the liver regeneration in the PHPL group was delayed and weak. In addition, there was reciprocal expression of C/EBPα and C/EBPβ mRNAs, an observation supported by their nuclear protein levels. Furthermore, the cytochrome P-450 protein level in the PHPL group was higher than that in the PH group 1 day after hepatectomy. ***Conclusion:*** The portal blood flow regulates the activity of liver regeneration and the gene expression associated with cell cycle regulators, while the functions are maintained.

Introduction

The unique ability of the liver to regenerate after partial loss due to surgery has long been recognized. Years of research have provided insights into the mechanism by which the fine interplay among cytokines and growth factors tightly regulates the liver regeneration [1–3]. The

KARGER
Fax +41 61 306 12 34
E-Mail karger@karger.ch
www.karger.com

0014–312X/06/0386–0522$23.50/0

Accessible online at:
www.karger.com/esr

Toru Mizuguchi, MD, PhD
Department of Surgery I, Sapporo Medical University Hospital
S-1, W-16, Chuo-Ku
Sapporo 060-8543 (Japan)
Tel. +81 11 611 2111 (ext. 3281), Fax +81 11 613 1678, E-Mail tmizu@sapmed.ac.jp

present-day knowledge of liver regeneration is derived mostly from the rodent model of partial (two-thirds) hepatectomy [1, 2], although the initial signals are still largely unknown. Once the liver starts to regenerate, a molecular cascade will follow the initial unknown signal. Cell signals of the IL-6/STAT pathway and of the HGF/c-met pathway have been proposed to play important roles in liver regeneration [1–4]. Following activation of these signals, cyclins play a major role in the progression of the cell cycle during liver regeneration [2, 3, 5]. Hepatocyte survival factors such as cardiotropin-1 (CT-1) also protect hepatocytes from death signals and surgical damage during liver regeneration [6]. In addition to these molecules, reciprocal expression of C/EBPα and C/EBPβ (CCAAT/enhancer-binding proteins) regulates the fundamental transcription of liver-specific genes to cause hepatocytes to proliferate and maintain their functions [3, 7, 8]. Although the molecular events in liver regeneration are well characterized after its initiation, the earliest signal or stimulus is still not known.

The portal pressure increases immediately after hepatectomy and generates shear stress in the remnant liver [9]. The shear stress after partial hepatectomy has been proposed to regulate liver regeneration, including hepatocyte proliferation and death [9, 10]. The activity of liver regeneration usually depends on the volume of the liver resection which increases shear stress in parallel with the increment of portal pressure. Splenectomy is one strategy to reduce portal blood flow after hepatectomy and could reduce mortality and facilitate liver regeneration [11]. A portocaval shunt is another method to reduce portal blood flow and facilitate liver regeneration in small-for-size graft syndrome [12]. Therefore, the portal blood flow plays an important role in determining the fate of liver regeneration; however, the molecular mechanism by which it regulates liver regeneration remains largely unknown.

We developed a simple rat model of partial portal ligation combined with partial hepatectomy to investigate the mechanism by which portal blood flow regulates liver regeneration and affects gene expression. This model was not a fatal model; therefore, it allowed us to obtain constant results and to investigate the simplest effect of portal blood flow on liver regeneration. We assumed that the liver would regenerate slowly and maintain the original function, if the portal flow changes were minimal after hepatectomy. Therefore, we focused on the molecular mechanism by which different degrees of portal blood flow regulate gene expression during liver regeneration.

Materials and Methods

Our animal studies were performed in compliance with institutional and National Research Council guidelines for humane care of laboratory animals.

Animals

Adult male Sprague-Dawley rats (250–350 g) were obtained from the Shizuoka Laboratory Animal Center (Hamamatsu, Japan). They were housed in a temperature-controlled (21 °C) room under a 12-hour light-dark cycle and were given tap water and standard laboratory chow. All operations were performed between 09.00 and 12.00 h under general (ether) anesthesia using a sterile surgical technique.

Surgical Animal Models

Partial Hepatectomy (PH). The two anterior liver lobes were removed as previously described [4]. In this model, removal of the two anterior lobes (68% of the liver) is known to induce the optimal proliferative response in the remnant liver mass.

PH with Partial Portal Ligation (PHPL). Preceding PH, the main portal vein between the first branch to the right liver lobe and the gastroduodenal vein was sutured with 8-0 Prolene to reduce the diameter by 40% (fig. 1a) with the aid of an operating microscope (Zeiss, Thornwood, N.Y., USA). The portal main trunk was clamped with microvascular clips and sutured twice with 2 mm space between the sutures (fig. 1b). The suturing bite was 40% of the clamped portal vein which reduced the portal diameter by 40%. In the unligated model, there were two sutures on the serosa of the portal vein without stricture.

Experimental Design

Groups of PH and PHPL rats were euthanized in batches of 6 animals 1, 3, 5, 7, and 14 days after surgery. One hour before euthanasia, 5-bromo-2′-deoxyuridine (BrdU) was injected intraperitoneally (50 mg/kg) [5]. When the animals were killed, part of the liver tissue was immediately frozen in liquid nitrogen for molecular analysis and part of it dipped into cold ethanol for immunohistochemical study.

Measurement of Hepatic Tissue Blood Flow (HTBF)

The HTBF was measured before and 5 min after surgery using a laser-Doppler flowmeter (ALF21; Advance, Tokyo, Japan) during the operation [13]. The probe of the flowmeter was placed on the surface of the right lobe of the liver. The measurement was continued for at least 3 s and repeated three times in 6 different rats.

Restitution of Liver Mass

The growth of the residual liver lobes (right and omental lobes) was calculated as the ratio liver weight/body weight.

BrdU Labeling Index (LI)

The proliferative activity in the liver after hepatectomy was determined by measuring the incorporation of BrdU, as previously described [8]. Briefly, a mouse anti-BrdU antibody (×100 dilution; Dako, Glostrup, Denmark) was used as the primary antibody, followed by the avidin-biotin complex method (Dako, Carpinteria, Calif., USA). Both labeled and unlabeled hepatocytes were counted in 20 fields in three different sections per time point

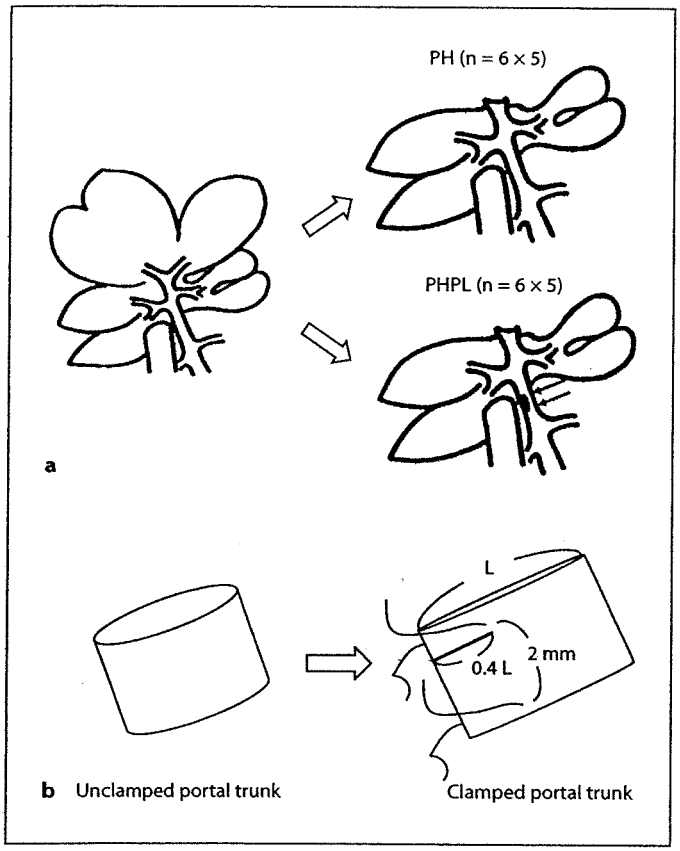

Fig. 1. a Surgical models of PH and PHPL. PH and PHPL rats were euthanized in batches of 6 animals 1, 3, 5, 7, and 14 days after surgery. **b** The portal trunk was clamped with microvascular clips to control portal blood flow. The portal trunk was sutured twice with 8-0 Prolene with a bite length of 40% of the total flattened portal width (L). This reduced the portal diameter by 40%.

from 5 different animals. Data are presented as mean values ± SD from three independent experiments.

Reverse Transcription-Polymerase Chain Reaction (RT-PCR)

Total RNA was extracted according to the Trizol protocol (Gibco-BRL Life Technologies, Gaithersburg, Md., USA). Single-strand complementary DNA was synthesized using an Omniscript RT kit (Quiagen, Valencia, Calif., USA) using the oligo-dT primer (Invitrogen, Carlsbad, Calif., USA). PCR primers were synthesized for CT-1 (5′-AGC ATG AGC CAG AGG GAG GGA A-3′ and 5′-TAT GCA GAC CAA TTG CTG GAG GAA-3′) [6], cyclin D (5′-TGA TAC CTG TGC TTT ATC CC-3′ and 5′-AAA CCA GCA TCT CTC TAA AC-3′) [14], cyclin E (5′-CTG ACC ATT GTG TCC TGG CT-3′ and 5′-CAG CTT GGA CTT GCT GGA CA-3′) [15], cyclin B (5′-TGA TAC CTG TGC TTT ATC CC-3′ and 5′-AAA CCA GCA TCT CTC TAA AC-3′) [14], C/EBPα (5′-GAA TCT CCT AGT CCT GGC TC-3′ and 5′-GAT GAG AAC AGC AAC GAG TAC-3′) [16], C/EBPβ (5′-GCC ACG GAC ACC TTC GAG G-3′ and 5′-CGG CTC CGC CTT GAG CTG-3′) [16], and glyceraldehyde-3-phosphate dehydrogenase (G3PDH; Clontech Laboratories, Palo Alto, Calif., USA). A Taq PCR kit (Takara Bio, Otsu, Japan) was used for all PCR reactions.

Western Blot Analysis

Western blot analysis was performed as described earlier [8]. Briefly, proteins were extracted using the NE-PER nuclear and cytoplasmic extraction protocol (Pierce Biotechnology, Rockford, Ill., USA). A BCA protein assay kit (Pierce Biotechnology) was used to measure the protein concentrations. Proteins (5 μg/lane) were separated on 10% Tris-HCl ready gel (Bio-Rad Laboratories, Hercules, Calif., USA), and the gel was further transferred to a nitrocellulose membrane (Amersham, Little Chalfont, UK), using a semidry blotting system (Bio-Rad Laboratories). The membrane was blocked overnight at 4°C with 5% dry milk, 0.05% Tween 20, and phosphate-buffered saline. Thereafter, it was incubated with anti-C/EBPα and anti-C/EBPβ (Santa Cruz Biotechnology, Santa Cruz, Calif., USA) and anti-rat CYP 1A1 and anti-rat CYP 3A2 (Daiichi Pure Chemicals, Tokyo, Japan) at room temperature for about 1 h, followed by a 30-min incubation with a horseradish-peroxidase-conjugated secondary (anti-rabbit or anti-goat IgG) antibody (Santa Cruz Biotechnology). The dilution for the primary antibody was 1:500 and for the secondary antibody 1:2,000. The ECL Western blotting analysis system (Amersham) was used to detect signals.

Densitometric Analysis

Scanning densitometry was performed using a Macintosh G4 computer (Apple Computer, Cupertino, Calif., USA) and an EPSON GT-9600 scanner (Seiko Epson, Suwa, Japan). The signals were quantified using the NIH Image 1.55 Densitometric Analysis Program [17].

Satatistics

Unpaired Student's t test, Welch's t test, or one-way analysis of variance were used, as appropriate. Data are given as mean values ± SD. The StatView 5.0 program (SAS Institute, Cary, N.C., USA) was employed, and the differences between mean values were considered significant, if $p < 0.05$.

Results

All rats tolerated the operative procedure well and recovered uneventfully from anesthesia.

HTBF in Residual Liver Lobes

Flow Doppler probes were placed on the right liver surface. The HTBF was measured with or without clamping of total blood flow to the liver before and immediately after the operation (fig. 2a). The HTBF in both PH and PHPL groups increased immediately after surgery. The HTBF in the PH group increased significantly more than that in the PHPL group (150.94 ± 11.08 vs. 114.52

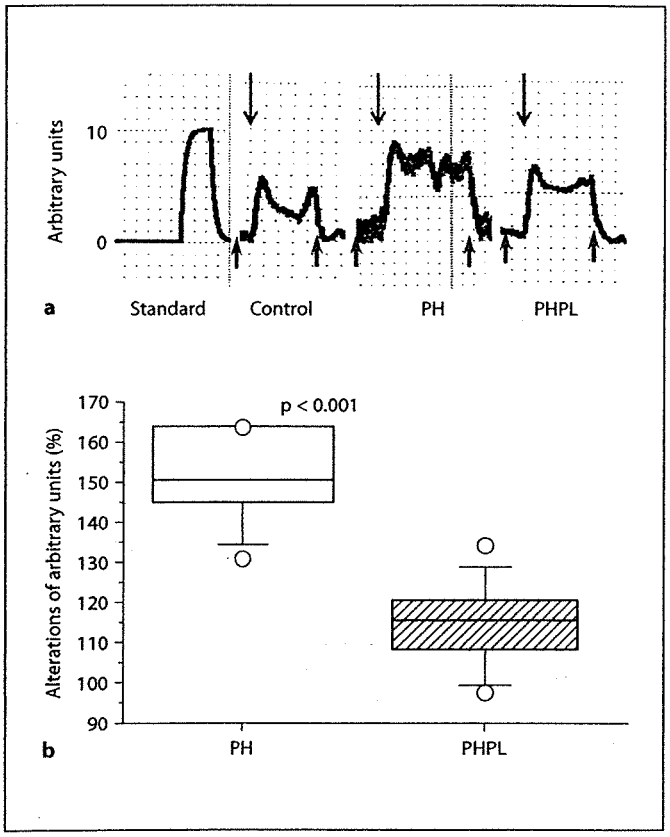

2

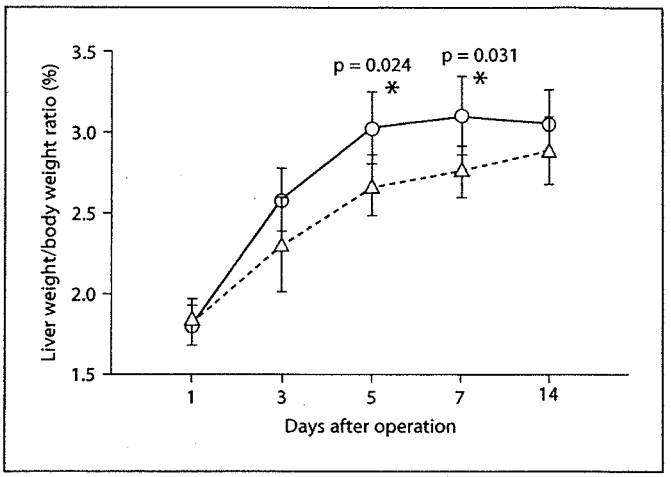

3

Fig. 2. HTBF laser-Doppler blood flowmetry. **a** HTBF was measured before surgery as a control and after PH and PHPL. A standard curve was obtained with 10 arbitrary units before the measurements. The long arrows indicate the clamped portal trunk and the short arrows the unclamped portal trunk. **b** Box plot analysis for the alterations of HTBF in the PH group (open box) and in the PHPL group (shaded box) 5 min after hepatectomy ($p < 0.001$).

Fig. 3. The ratio liver weight/body weight shows restitution of the remnant liver. ○ = PH group; △ = PHPL group. The asterisks indicate statistical significant differences between the groups ($p < 0.05$).

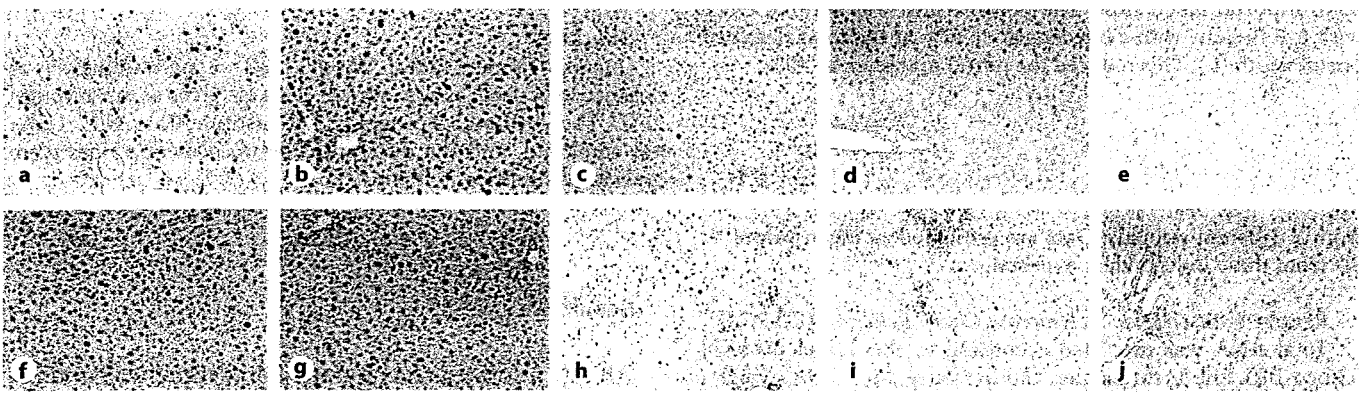

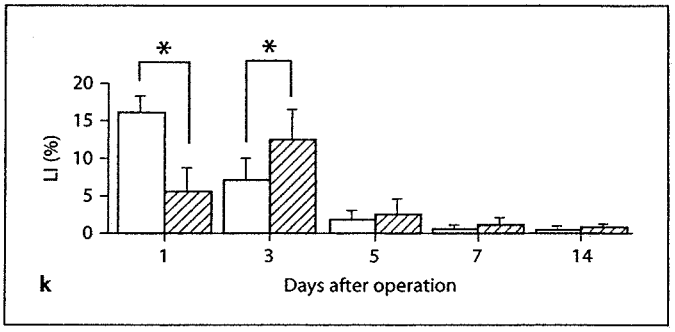

Fig. 4. Immunohistochemistry of BrdU staining in the PH group (**a**–**e**) and in the PHPL group (**f**–**j**) on day 1 (**a**, **f**), day 3 (**b**, **g**), day 5 (**c**, **h**), day 7 (**d**, **i**), and day 14 (**e**, **j**). The dark gray nuclei are positive for BrdU. **k** The LIs were calculated from 20 fields in three different sections per time point from 5 animals. Open columns: PH group; hatched columns: PHPL group. * $p < 0.01$.

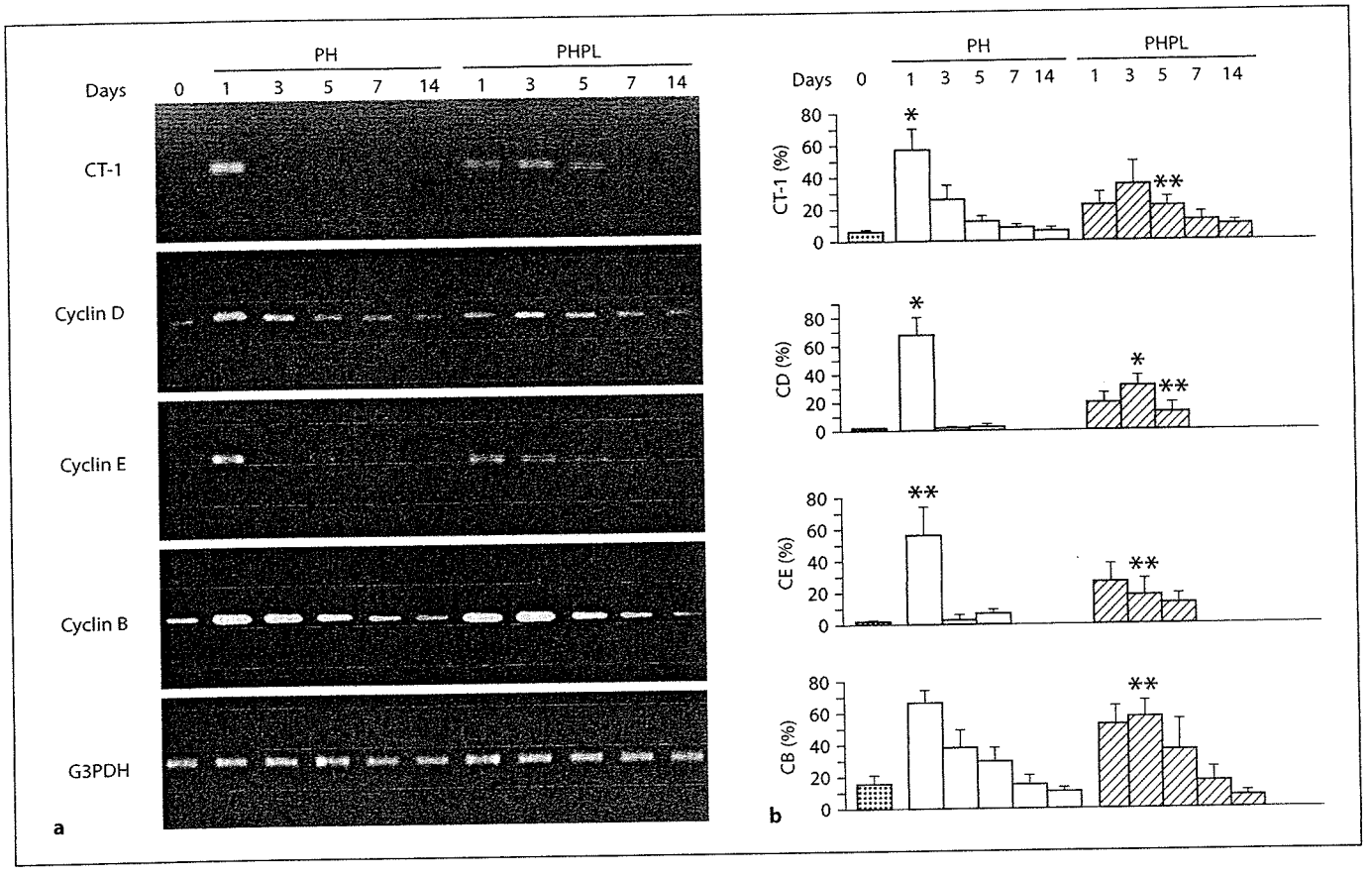

Fig. 5. a RT-PCR for CT-1, cyclin D, cyclin E, cyclin B, and G3PDH mRNA expression in the PH and PHPL groups. **b** Densitometric analysis of the PCR signals. All the densitometric data show relative signals of the PCR product compared to that of G3PDH mRNA expression in the same sample cDNA. Dotted columns: normal rats before surgery; open columns: PH group; hatched columns: PHPL group. The data were significantly different between the groups at the same time point: * $p < 0.01$; ** $p < 0.05$.

± 10.89%; $p < 0.001$), indicating that the microcirculation in the PHPL group immediately after hepatectomy was much lower than that in the PH group.

Growth of Liver Remnants

To evaluate the recovery of the remnant liver, the rats were euthanized, and liver volume and body weight were determined (fig. 3). The ratio of the remnant liver lobes to the body weight on day 1 showed no difference between the groups. It linearly increased in the PH group after day 1, whereas it slowly increased in the PHPL group. Although there was no difference in the sequential variation between the groups ($p = 0.245$), there were significant differences between the groups on days 5 and 7: 3.03 ± 0.22 vs. 2.67 ± 0.19% ($p = 0.024$) and 3.11 ± 0.26 vs. 2.76 ± 0.16% ($p = 0.031$), respectively.

BrdU Immunohistochemistry and LI

We found that partial ligation of the portal vein affected residual HTBF and recovery of the liver weight/body weight ratio after partial hepatectomy. Next, we conducted immunohistochemistry for BrdU and calculated the LI at each time point to investigate the activity of hepatocyte proliferation during liver regeneration (fig. 4). In the PH group, peak BrdU uptake was seen 1 day after hepatectomy, and it decreased subsequently (fig. 4a–e), whereas in the PHPL group, peak BrdU uptake was delayed to day 3 (fig. 4f–j) and prolonged. The LI (fig. 4k) on day 1 in the PH group was significantly higher than that in the PHPL group (16.18 ± 1.39 vs. 5.61 ± 2.01%; $p < 0.01$), whereas on day 3 in the PH group, the LI was significantly lower than that in the PHPL group (7.08 ± 1.89 vs. 12.45 ± 2.57%; $p < 0.01$).

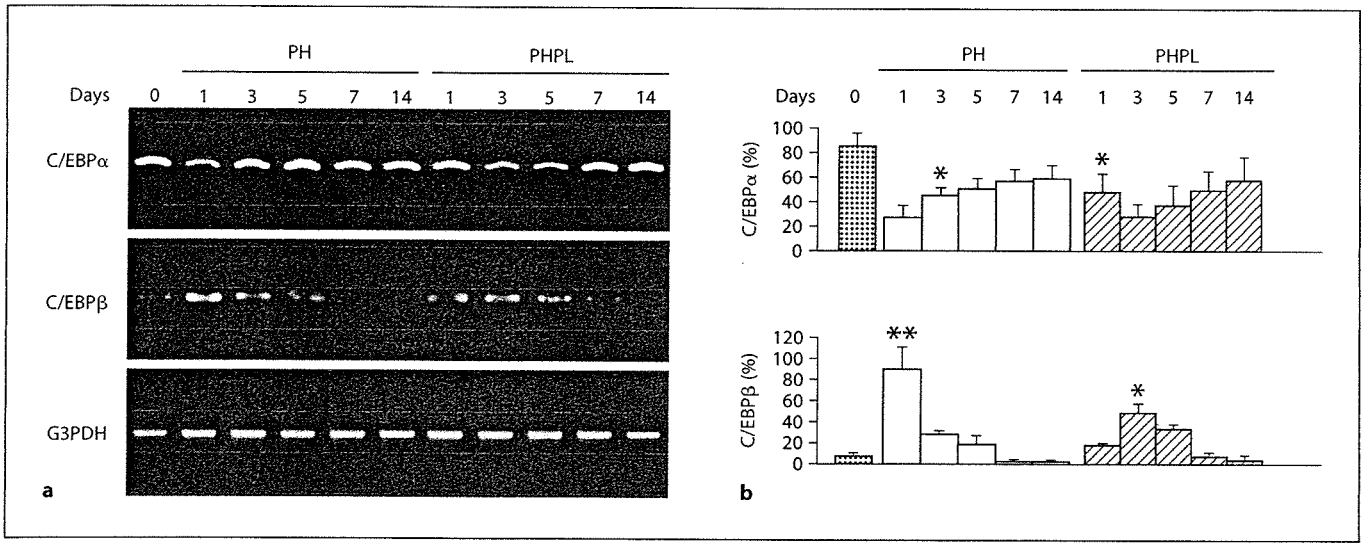

Fig. 6. a RT-PCR for C/EBPα, C/EBPβ, and G3PDH mRNA expression in the PH and PHPL groups. **b** Densitometric analysis of PCR signals. All the densitometric data show relative signals of the PCR product compared to that of G3PDH mRNA expression in the same sample cDNA. Dotted columns: normal rats before surgery; open columns: PH group; hatched columns: PHPL group. The data were significantly different between the groups at the same time point: * $p < 0.05$; ** $p < 0.01$.

Cell-Cycle-Associated Gene Expression during Liver Regeneration

We found that the hepatocyte proliferation was delayed and prolonged in the PHPL model. We examined the gene expression associated with liver regeneration (fig. 5). The mRNA expression of CT-1 in the PH group was strikingly elevated on day 1 and then decreased, whereas in the PHPL group it was delayed and weak during the experiment. The mRNA expression of cyclins D and E in the PH group was strikingly elevated on day 1 and dropped thereafter, whereas in the PHPL group it was delayed and weak with a peak of slight expression on day 3. The mRNA expression of cyclin B in the PH group was also elevated on day 1 and then decreased gradually, whereas in the PHPL group it was elevated on day 3 and decreased on day 5.

Reciprocal Expression of C/EBPα and C/EBPβ in Liver Regeneration

Liver-enriched transcription factors such as HNFs and C/EBPs regulate hepatocyte proliferation and function. C/EBPα and C/EBPβ, in particular, play very important roles in inducing hepatocytes to proliferate and to maintain innate functions. Therefore, we examined the C/EBPα and the C/EBPβ mRNA expression (fig. 6) and protein levels (fig. 7) during the experiment.

The C/EBPα mRNA expression in the PH group strikingly dropped on day 1 (27.22 ± 9.81%) and gradually increased. On the other hand, the C/EBPα mRNA expression in the PHPL group decreased by day 3 (50.17 ± 13.76% on day 1 and 28.87 ± 9.15% on day 3). The C/EBPβ mRNA expression in the PH group increased on day 1 (90.05 ± 20.51%) and decreased thereafter, whereas in the PHPL group it was slightly elevated, and the peak of the expression was seen on day 3 (50.96 ± 13.58%).

The protein level of C/EBPα in the PH group decreased on day 1 (26.44 ± 11.24%) and gradually recovered. On the other hand, in the PHPL group it decreased by day 3 (30.28 ± 9.75%) and increased gradually thereafter. The protein level of C/EBPβ in the PH group increased on day 1 (355.42 ± 96.08%) and subsequently dropped after day 3 to the normal level. On the other hand, in the PHPL group it increased on day 3 (304.52 ± 100.69%), and the high level was maintained on day 5 (234.25 ± 89.07%), but otherwise remained at almost the normal level.

Cytochrome P-450 (CYP) 1A1 and 3A2 Expression in Liver Regeneration

CYP proteins decrease during liver regeneration, in association with hepatocyte proliferation and liver func-

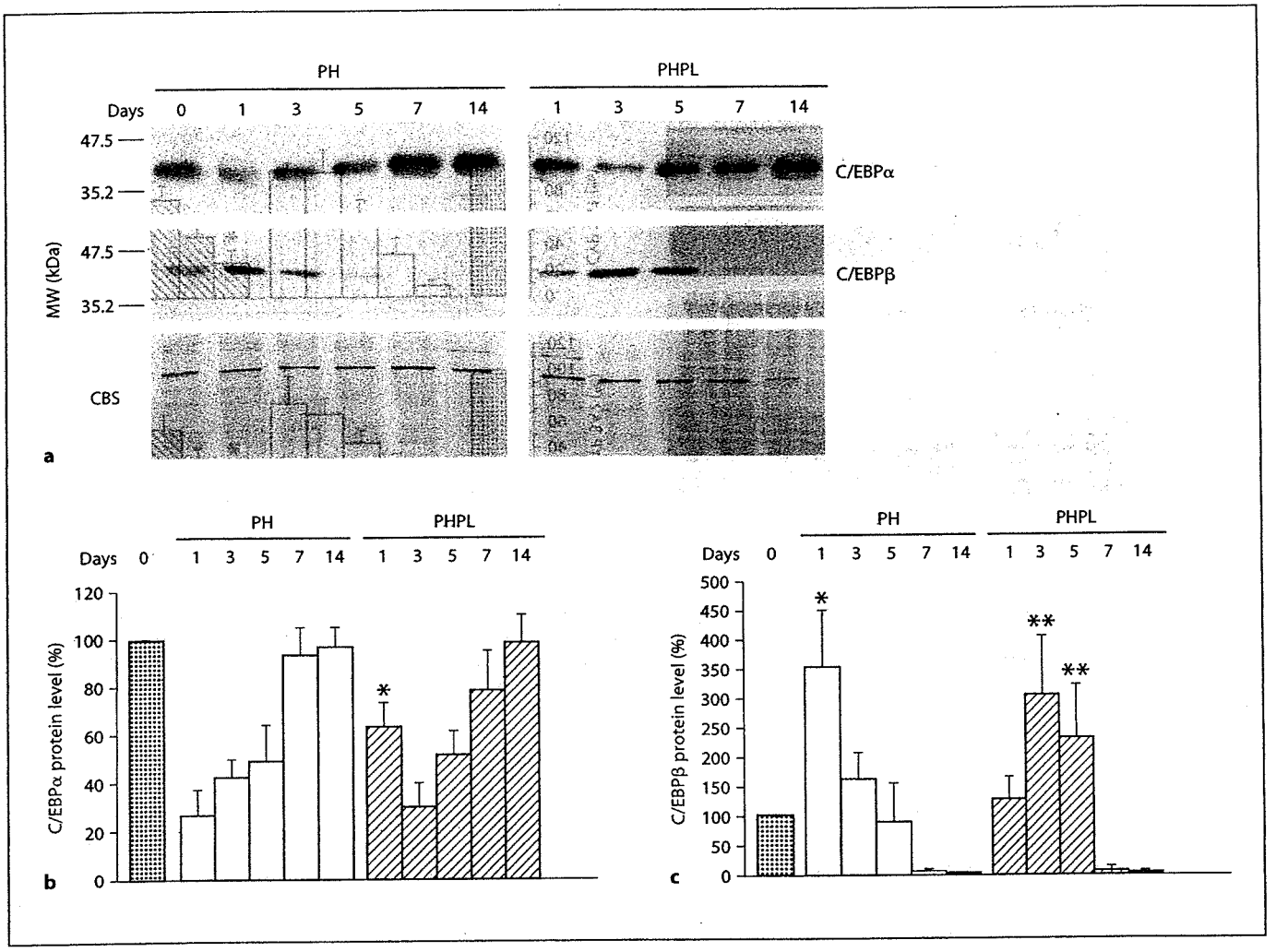

Fig. 7. a Western blot analysis for C/EBPα and C/EBPβ in the nuclear protein in PH and PHPL groups. Nuclear protein (5 μg) was applied in each lane. Coomassie blue staining (CBS) is an internal control of the sample. **b, c** Densitometric analysis of C/EBPα (**b**) and C/EBPβ (**c**) protein signals. Dotted columns: normal rats before surgery; open columns: PH group; hatched columns: PHPL group. The data were significantly different between the groups at the same time point: * $p < 0.01$; ** $p < 0.05$.

tional deterioration. Although the expression of both CYP1A1 and CYP3A2 proteins did not differ between the groups after 3 days or later (fig. 8), both protein levels 1 day after hepatectomy were higher in the PHPL group than in the PH group: 26.91 ± 9.85 vs. 8.12 ± 4.32% ($p = 0.02$) and 23.78 ± 7.42 vs. 6.18 ± 3.32% ($p < 0.01$), respectively. That is, the reduction of the CYP proteins in the PHPL group after hepatectomy was at a lower level than that in the PH group.

Discussion

We developed a simple model to investigate the effect of HTBF on liver regeneration. The HTBF affected liver regeneration with regard to morphology and gene expression. The reduction of portal flow weakened hepatocyte proliferation and delayed it which was supported by the expression of all the genes examined.

Surgical Model to Investigate the HTBF

The portal flow is well known to play an important role in liver regeneration [9, 18]. In fact, we encountered

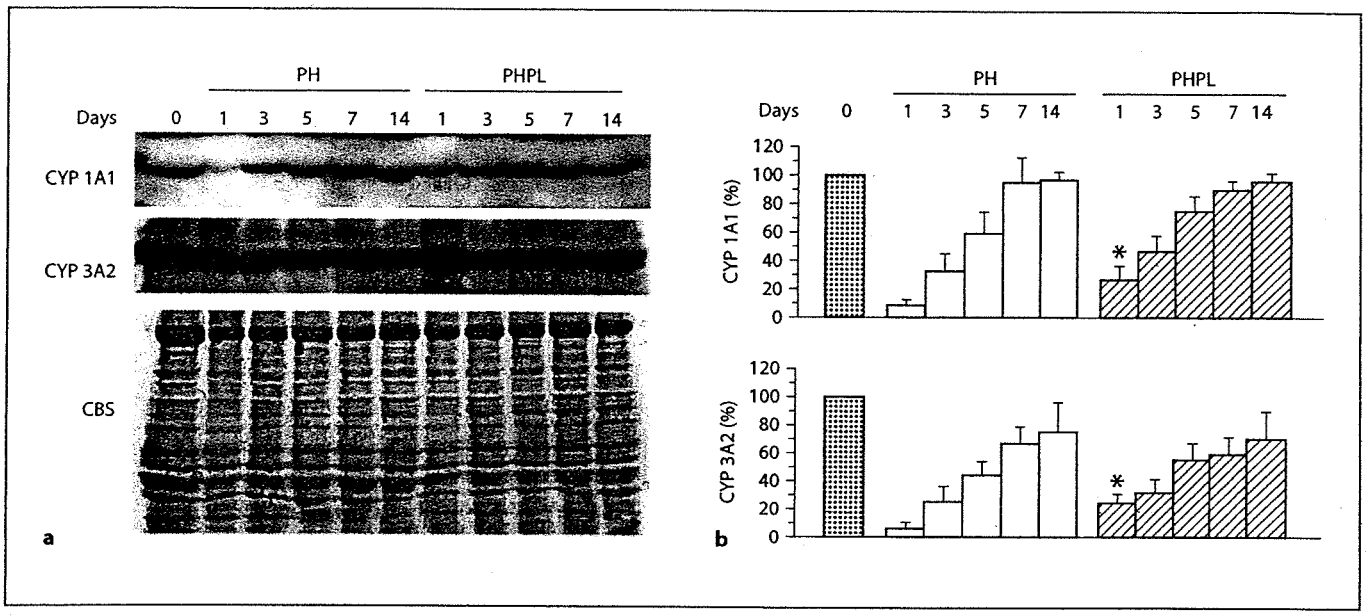

Fig. 8. a Western blot analysis for CYP 1A1 and CYP 3A2 in the PH and PHPL groups. Protein (20 μg) was applied in each lane. Coomassie blue staining (CBS) is an internal control of the sample. **b** Densitometric analysis of protein signals. Dotted columns: normal rats before surgery; open columns: PH group; hatched columns: PHPL group. The data were significantly different between the groups at the same time point: * $p < 0.01$.

many cases in which excessive blood flow caused liver failure after extended liver resection or after using small-for-size grafts in living-donor liver transplantation. Reduction of the liver blood flow caused by transposition of the spleen [19] or a portal systemic shunt [20] has been shown to reduce the risk of liver failure and to increase survival rates after extensive hepatectomy in rodent models. However, the lack of a simple model for investigating blood flow in liver regeneration has led to failure to understand the exact molecular mechanism by which hepatic blood flow regulates the liver regeneration.

We developed a simple model to observe the effect of hepatic blood flow on liver regeneration. In this model, the volume of liver resection was the same, and the only difference was in the portal blood flow immediately after hepatectomy. As we have shown, reduction of the HTBF delayed the recovery of liver volume with less DNA synthetic activity and affected gene expression to maintain the CYP protein level in the liver during regeneration. Although the difference of HTBF caused by partial ligation of the portal vein may have lasted only for a short period after the operation, the initial HTBF affected liver regeneration and functions associated with gene expression. Recently, Marubashi et al. [21] developed a novel model to investigate the effect of portal blood flow on liver regeneration. They also found that liver generation was attenuated in the low portal pressure model, although the pressure difference did not last for more than 12 h. The early events they reported are consistent with our results.

Hepatic Blood Flow after Hepatectomy

The hepatic blood inflow was both arterial flow and portal flow. Once the portal flow decreases for any reason, arterial flow compensates to maintain the hepatic blood supply [22]. Reduction of the portal inflow increases the arterial flow which is well known as the hepatic arterial buffer effect. In fact, a portal branch ligation murine model [18] showed that the liver regenerates with arterial flow compensation. Furthermore, temporal reduction of the portal flow increases the arterial flow in human liver transplantation [23]. It is difficult to differentiate the portal and arterial flow stimulation in liver regeneration after hepatectomy. Therefore, we should study the tissue blood flow supply, as we have done in this work, instead of measuring each blood flow. The flow measured using laser-Doppler scanning has been shown to correlate with the actual blood flow in the brain [24]. Unfortunately, it is uncertain whether the flow measured using laser-Doppler scanning in the liver correlated with